ISTANBUL TECHNICAL UNIVERSITY ★ GRADUATE SCHOOL

DEVELOPMENT OF NOVEL INHIBITORS TARGETING DRP1-MID49/51 INTERACTION AT MITOCHONDRIAL FISSION

M.Sc. THESIS

Behnaz GHADERKALANKESH

Department of Computer Sciences

Computer Sciences Programme

APRIL 2022

ISTANBUL TECHNICAL UNIVERSITY ★ GRADUATE SCHOOL

DEVELOPMENT OF NOVEL INHIBITORS TARGETING DRP1-MID49/51 INTERACTION AT MITOCHONDRIAL FISSION

M.Sc. THESIS

Behnaz GHADERKALANKESH
(704181005)

Department of Computer Sciences

Computer Sciences Programme

Thesis Advisor: Assist. Prof. Sefer BADAY

APRIL 2022

İSTANBUL TEKNİK ÜNİVERSİTESİ ★ LİSANSÜSTÜ EĞİTİM ENSTİTÜSÜ

MİTOKONDRİYAL FİZYON MEKANİZMASINDAKİ DRP1-MID49/51 ETKİLEŞİMİNİ HEDEF ALAN İNHİBİTÖR GELİŞTİRİLMESİ

YÜKSEK LİSANS TEZİ

Behnaz GHADERKALANKESH
(704181005)

Bilgisayar Bilimleri Anabilim Dalı

Bilgisayar Bilimleri Programı

Tez Danışmanı: Assist. Prof. Sefer BADAY

NİSAN 2022

Behnaz GHADERKALANKESH, a M.Sc. student of ITU Graduate School student ID 704181005 successfully defended the thesis entitled "DEVELOPMENT OF NOVEL INHIBITORS TARGETING DRP1-MID49/51 INTERACTION AT MITOCHONDRIAL FISSION", which she prepared after fulfilling the requirements specified in the associated legislations, before the jury whose signatures are below.

Thesis Advisor :	**Assist. Prof. Sefer BADAY** Istanbul Technical University	.....
Jury Members :	**Assoc. Prof. Onur ALPTÜRK** Istanbul Technical University	.....
	Assist. Prof. Özge ŞENSOY Medipol University	.....
		.....

Date of Submission : **20 April 2022**
Date of Defense : **29 April 2022**

FOREWORD

First of all, I would like to express my gratitude and appreciation to my advisor, prof. Sefer BADAY. Thank you so much for being an incredible advisor.
I also want to present my special thanks to my husband, parents and sisters for their support and patience throughout the duration of this thesis.

April 2022 Behnaz GHADERKALANKESH

TABLE OF CONTENTS

ABBREVIATIONS

ADME/T	**:** Absorption, distribution, metabolism, and excretion/toxicity
ATP	**:** Adenosine Triphosphat
ADT	**:** AutoDock Tools
Vina	**:** AutoDock Vina
DRP1	**:** Dynamin-related protein 1
XP	**:** Extra-precision
MAE	**:** Meastro file format
MiD49	**:** Mitochondrial dynamics protein MID49
MiD51	**:** Mitochondrial dynamics protein MID51
MOM	**:** Mitochondrial Outer Membrane
MD	**:** Molecular Dynamics
PDB	**:** Protein data bank
PDBQT	**:** Protein data bank, partial charge & atom type
RMSD	**:** Root-mean-square deviation
SMI	**:** SMILES format

SYMBOLS

$^{\circ}$**K**	**:**Kelvin
Å	**:**Angstrom

LIST OF TABLES

Page

LIST OF FIGURES

DEVELOPMENT OF NOVEL INHIBITORS TARGETING DRP1-MID49/51 INTERACTION AT MITOCHONDRIAL FISSION

SUMMARY

Mitochondria are responsible for the production of the majority of our energy known as Adenosine Triphosphate(ATP). Energy production is the best-known role of mitochondria but they are responsible for other important tasks as well. Mitochondrial fission and fusion are necessary process for naturally dynamic mitochondria. Mitochondrial dysfunction plays a significant role in the development and progression of several diseases such as cancer and diabetes.

Mitochondria continually undergo shape and number changes by fission and fusion. Cytoplasmic GTPase Dynamin-related protein 1 (DRP1) regulates mitochondrial fission. It is a protein, part of the dynamin family which is made up of an N-terminal GTPase domain and a C-terminal GTPase effector domain. MiD49 and MiD51 are mitochondrial dynamics proteins linked to the mitochondrial outer membrane. These two proteins directly recruit Drp1 protein to the mitochondrial membrane to form a ring around and start the fission process.

Recent studies have shown that cancer tumors alter mitochondrial dynamics to resist apoptosis by causing fission protein, Dynamin-related protein 1 (DRP1) to overexpress. In addition, this is the cause of neurodegenerative and diabetes type 1 disorders. As a result, designing new inhibitors will have a great impact on finding ways to overcome mitochondrial disorders.

While there have been many molecular docking studies about Drp1-MiD49/51 inhibition recently, in order to design small molecules that can be utilized as drugs, and not have side effects like Mdivi1 and Dynasore we performed this study in a specific way.

Molecular docking calculation is an important approach in the field of drug design and discovery which is used when we want to predict a ligand-receptor complex structure. Docking is accomplished in two phases that are intertwined. First, sampling the structure of the ligand, as well as its position and orientation inside the protein's active site, and then these created conformations will be ranked among all conformations by a scoring function [1].

Structure-based virtual screening (SBVS), also known as target-based virtual screening (TBVS), is a computational technique used in drug discovery which computationally screens a library of small molecules against a target to identify the best binding and high scored molecules [2].

This study comprises two phases, first phase uses computational approaches that may improve resource utilization and speed drug development, and in the second phase,

found novel compounds will be synthesized for further steps. In this thesis, the main focus will be on the computational phase of the work.

Here we aim to inhibit DRP1-MiD49/MiD51 proteins interaction in several ways. In the first packet, we tried to design new inhibitors targeting the DRP1-GTPase nucleotide-binding domain. For this goal, docking calculations were performed in several stages. To start docking calculations, 3.5 million, in-stock, lead-like small molecules from the ZINC database were used.

Autodock vina, Ledock and Schrodinger Glide(XP) programs were used in different steps for docking calculations [3]–[5]. The reason for choosing these three programs was their high performance in different studies so far. After docking calculations for 3.5 million molecules another step was performed which was the docking of the previous step's high scored molecules to DRP1 protein's off-target proteins and in the same way to DRP1 protein using Vina(exhaustiveness 24) and Ledock. In the next step, molecules with specific criteria were selected for docking using Glide XP and then clustering and ADME/T (absorption, distribution, metabolism, and excretion/toxicity) properties to select optimum ligands for their possible pharmaceutical use. As the final step of the first path, high-scored molecules from the previous step were selected for molecular Dynamic simulations to calculate binding free energy using the OSPL2005 force field and TIP3P water model of Schrödinger Desmond Software and MMGBSA calculations. Finally, 30 molecules were selected as the molecules with the highest free binding energies. In the second packet, every step in packet 1 was repeated identically for MiD49 and MiD51 proteins.

MİTOKONDRİYAL FİZYON MEKANİZMASINDAKİ DRP1-MID49/51 ETKİLEŞİMİNİ HEDEF ALAN İNHİBİTÖR GELİŞTİRİLMESİ

ÖZET

Mitokondriler, Adenozin Trifosfat (ATP) olarak bilinen enerjimizin çoğunun üretiminden sorumludur. Enerji üretimi mitokondrinin en iyi bilinen rolüdür ancak diğer önemli görevlerden de sorumludurlar. Mitokondriyal füzyon, doğal olarak dinamik mitokondri için gerekli bir süreçtir. Mitokondriyal disfonksiyon, kanser ve diyabet gibi çeşitli hastalıkların gelişmesinde ve ilerlemesinde önemli bir rol oynar.

Mitokondri sürekli olarak fisyon ve füzyon yoluyla şekil ve sayı değişikliklerine uğrar. Sitoplazmik GTPaz Dinaminle ilişkili protein 1 (DRP1) mitokondriyal fisyon düzenler. Bir N-terminal GTPaz alanından ve bir C-terminal GTPaz efektör alanından oluşan dinamin ailesinin bir parçası olan bir proteindir. MiD49 ve MiD51, mitokondriyal dinamik proteinlerdir ve mitokondriyal dış zarla bağlantılıdır. Bu iki protein, etrafında bir halka oluşturmak ve fisyon sürecini başlatmak için doğrudan Drp1 proteinini mitokondriyal membrana alır.

Son çalışmalar, kanser tümörlerinin, fisyon proteini, Dinaminle ilişkili protein 1'in (DRP1) aşırı eksprese olmasına neden olarak apoptoza direnmek için mitokondriyal dinamikleri değiştirdiğini göstermiştir. Ayrıca bu neden nörodejeneratif ve diyabet tip 1 bozukluklarının nedenidir. Sonuç olarak, yeni inhibitörler tasarlamanın mitokondriyal bozuklukların üstesinden gelmenin yollarını bulmada büyük etkisi olacaktır.

Hedefe dayalı sanal tarama (TBVS) olarak da bilinen yapı tabanlı sanal tarama (SBVS), en iyi bağlayıcı ve yüksek puanlı molekülleri belirlemek için küçük moleküllerden oluşan bir kitaplığı bir hedefe karşı hesaplamalı olarak tarayan ilaç keşfinde kullanılan bir hesaplama tekniğidir [2].

Bu çalışma iki aşamadan oluşmaktadır, ilk aşamada kaynak kullanımını iyileştirebilecek ve ilaç geliştirmeyi hızlandırabilecek hesaplama yaklaşımları kullanılmaktadır ve ikinci aşamada bulunan yeni bileşikler daha sonraki aşamalar için sentezlenecektir. Bu tezde asıl odak, çalışmanın hesaplama aşaması olacaktır.

Burada, DRP1-MiD49/MiD51 proteinlerinin etkileşimini çeşitli şekillerde engellemeyi amaçlıyoruz. İlk pakette, DRP1-GTPase nükleotid bağlama alanını hedefleyen yeni inhibitörler tasarlamaya çalıştık. Bu amaç için, yerleştirme hesaplamaları birkaç aşamada gerçekleştirilmiştir. Yerleştirme hesaplamalarını başlatmak için, ZINC veri tabanından 3,5 milyon, stokta bulunan, kurşun benzeri küçük moleküller kullanıldı.

Yerleştirme hesaplamaları için farklı adımlarda Autodock vina, Ledock ve Schrödinger Glide(XP) programları kullanılmıştır [3]–[5]. Bu üç programın seçilmesinin nedeni, bugüne kadar yapılan farklı çalışmalarda gösterdikleri yüksek performanstı. 3.5

milyon molekül için kenetlenme hesaplamalarından sonra, bir önceki adımın yüksek puanlı moleküllerinin DRP1 proteinin hedef dışı proteinlerine ve aynı şekilde Vina(tükenme 24) ve Ledock kullanılarak DRP1 proteinine kenetlenmesi olan başka bir adım gerçekleştirildi. Bir sonraki adımda, Glide XP ve ardından olası farmasötik kullanımları için optimum ligandları seçmek için kümeleme ve ADME/T (emilim, dağılım, metabolizma ve atılım/toksisite) özellikleri kullanılarak yerleştirme için belirli kriterlere sahip moleküller seçilmiştir. İlk yolun son adımı olarak, Schrödinger Desmond Yazılımının OSPL2005 kuvvet alanı ve TIP3P su modeli ve MMGBSA hesaplamaları kullanılarak bağlanma serbest enerjisini hesaplamak için moleküler Dinamik simülasyonlar için önceki adımdan yüksek puanlı moleküller seçildi. Son olarak, en yüksek serbest bağlanma enerjilerine sahip moleküller olarak 30 molekül seçilmiştir. İkinci pakette, paket 1'deki her adım MiD49 ve MiD51 proteinleri için aynı şekilde tekrarlandı.

1. INTRODUCTION

Mitochondria are essential organelles found in almost all eukaryotic cells. A double-membrane system surrounds mitochondria, with inner and outer mitochondrial membranes separated by an inter-membrane gap.

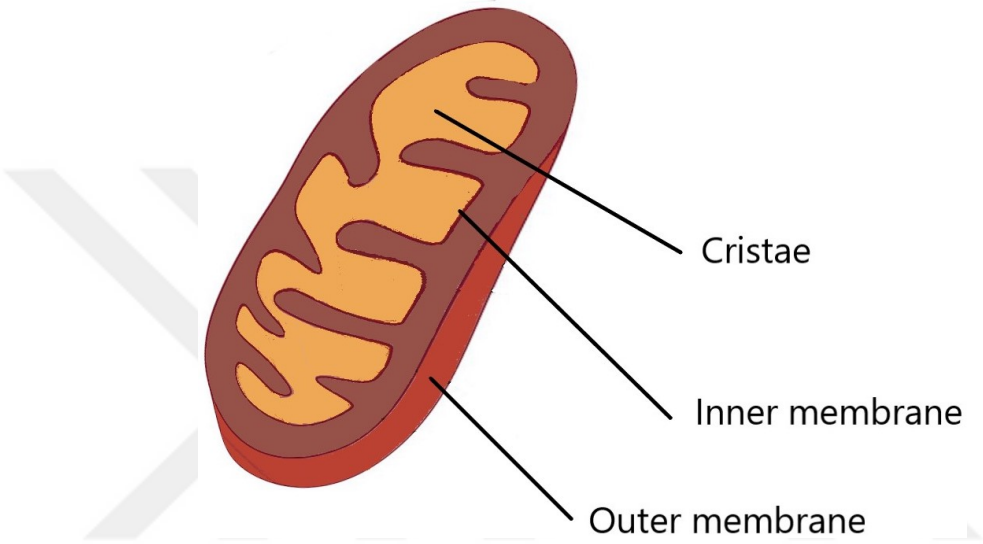

Figure 1.1 : Mitochondria structure

Mitochondria play a key role in human body. The most well-known role of mitochondria is the production of the energy in the form of ATP (Adenosine triphosphate) needed for cellular processes in the body. Nearly 90% of the energy needed for our body is produced by the mitochondria. This process involves converting chemical energy in the food we eat into the energy which can be used by our cells (Oxidative phosphorylation). Recently conducted researches have demonstrated that mitochondria are involved in several activities as well, which are vital for a well-functioning body like calcium homeostasis, programmed cell death, heat production, mitophagy, etc. Mitochondria's dysfunction leads to chronic diseases. Important symptoms of mitochondrial diseases include diabetes, cancer, Alzheimer, poor growth, heart and kidney diseases, etc [6].

Mitochondria have an outstanding responsibility in regulation of apoptosis (programmed cell death) [7]. Modulation of mitochondrial dynamics, such as fusion, fission and removal are regulated by mitochondrial proteins [8]. Mitochondrial fission is the division of a mitochondrion into two distinct mitochondria [9]. Mitochondrial fusion is mixing the content of the outer and then the inner mitochondrial membranes of two distinct mitochondria. Mitochondrial fusion is mostly governed by three GTPases: Mitofusin1 (Mfn1), Mfn2, and optic atrophy 1 (Opa1), while Drp1 promotes mitochondrial fission [10] [11]. Recent studies have shown that cancer tumors alter mitochondrial functions to resist apoptosis with causing fission protein, Dynamin-related protein 1 (Drp1) to overexpress due to promote tumor initiating and their survival [12]. Based on the Oncomine and TCGA datasets (https://www.cancer.gov/tcga), Drp1 was significantly overexpressed in lung cancer tissues. Furthermore, immunohistochemical results revealed that the level of Drp1 protein in lung cancer was substantially higher than that in matched normal tissues [13,14]. In addition, this reason is cause of neurodegenerative and diabetes tip 1 disorders. As a result, designing novel inhibitors will have a great impact on finding ways to overcome mitochondrial disorders.

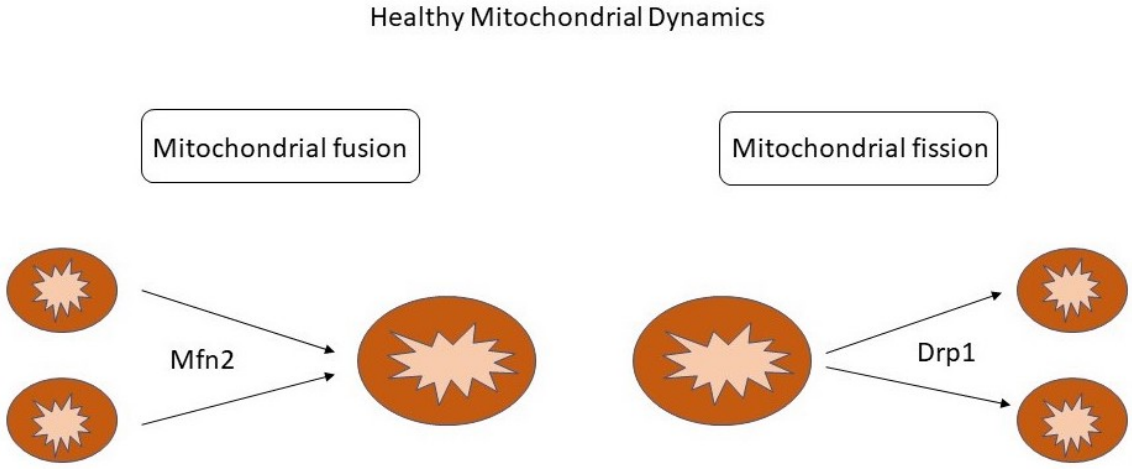

Figure 1.2 : Mitochondrial fusion and mitochondrial fission. Mfn2 gene promotes Mitochondrial fusion, while Drp1 promotes mitochondrial fission. If the ratio of Mfn2 and Drp1 is changed, there is abnormal increase in the fission which is the cause of mitophagy.

1.1 Drp1 structure and functions

A C-terminal GTPase effector domain, a variable domain (also known as insert B), a helical intermediate domain, and a highly conserved N-terminal GTPase domain are known to exist in the Drp1 protein. The variable domain functions as a hinge, generating a T-shaped dimer that easily binds the targeted membrane [15]. Drp1 does not contain a lipid-interacting domain, therefore it can only anchor to the mitochondrial membrane by binding to its receptor to create a functional complex, which is subsequently aggregated into a bigger oligomer and transported to fission sites. Drp1 is recruited to the MOM for fission by four mitochondrial outer membrane (MOM) receptors: mitochondrial dynamics protein 49 and 51 (MiD49 and MiD51), mitochondrial fission factor (Mff), and fission 1 receptor (Fis1) [16]. MiD49 and MiD51 are mitochondrial proteins that can both attract Drp1 to mitochondrial fission sites without the involvement of Fis1 or Mff [17]. Recent findings suggest that mitochondrial function and dynamics are intertwined and maintain the cellular and organismal balance between health and disease [18].

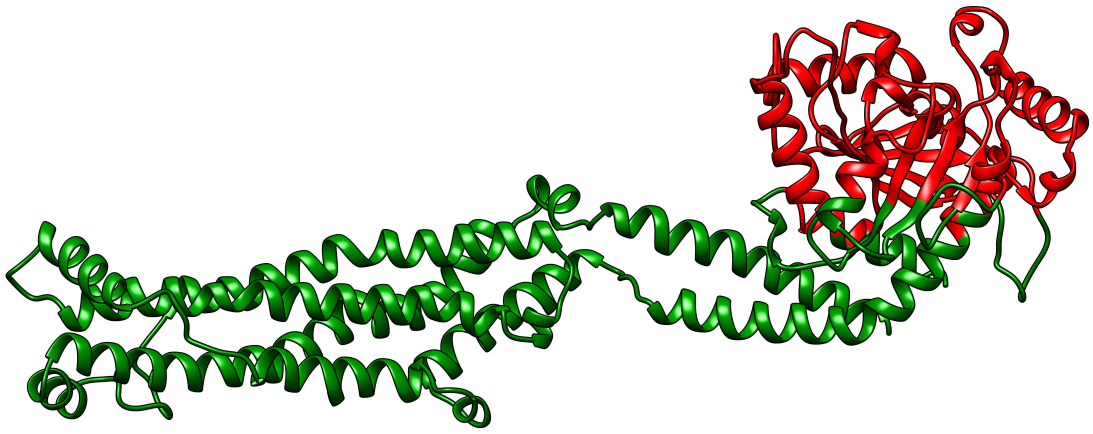

Figure 1.3 : The 3D structure of Drp1 (4BEJ) visualized in Chimera. Active site of Drp1 (4BEJ) is represented by red

Mitochondria are naturally dynamic organelles. They undergo different changes like fusion and fission which are necessary for a well-functioning metabolism and cell survival. Excessive mitochondrial division (fission), for example, is linked to functional abnormalities and has been linked to a variety of human disorders, including neurological diseases and cancer.

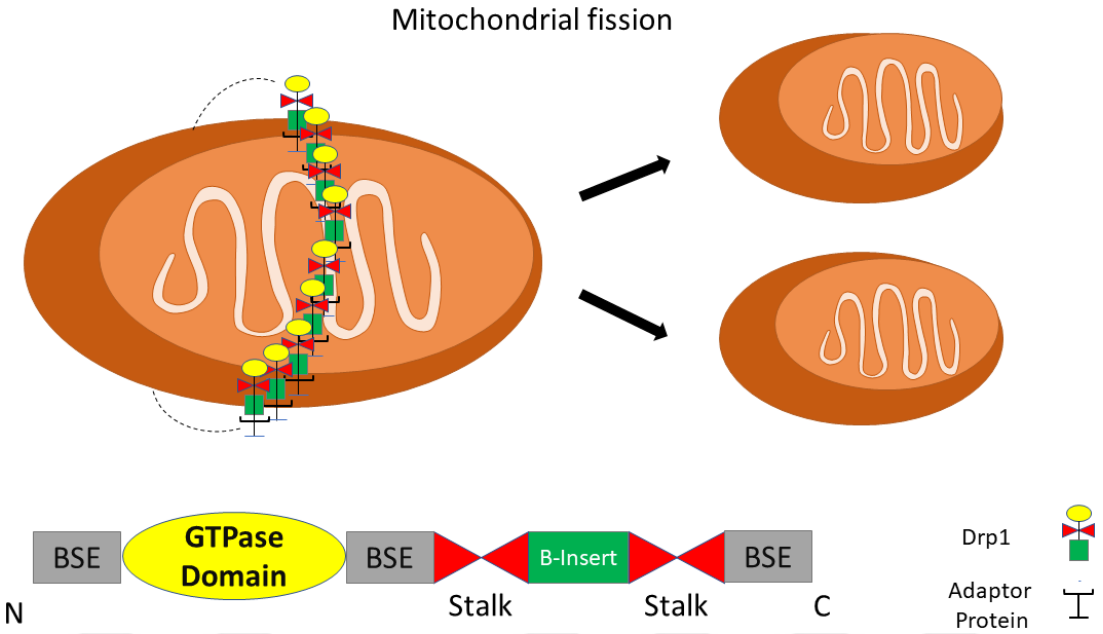

Figure 1.4 : DRP1 function in mitochondrial fission

1.2 MiD49 and MiD51 structure and functions

MiD49 and MiD51 are two mitochondrial outer membrane receptors with surface loop that can recruit Drp1 to aid mitochondrial fission. MiD51 possesses a variant nucleotidyl transferase structure that binds an ADP co-factor required for Drp1 function activation. MiD51 shares sequence homology with MiD49 [19].

3D structures of MiD49 and MiD51's sytosolic domains and complex forms exist. Therefore structure-based computational methods involved in drug discovery were used in this study. Despite having sequence identity more than 49% MiD49 and MiD51 do not bind same nucleotides (Richter vd., 2014).

In an attempt to identify novel inhibitors of Dynamin-related protein 1 (Drp1) and MiD49/51 anchored in the mitochondrial outer membrane with a key role in Drp1's localization in mitochondrial outer membrane, we performed a virtual screening for nearly 3.5 million molecules from ZINC database. In this study it was aimed to discover drug molecules which have significant binding potential to Drp1-GTPase domain and in a second step screening molecules which have binding potential to MiD49/51 proteins. In this regard multi-step Docking calculations using different

programs and several methods for reducing number of molecules were performed to achieve a shortlist of candidate molecules which can be synthesized.

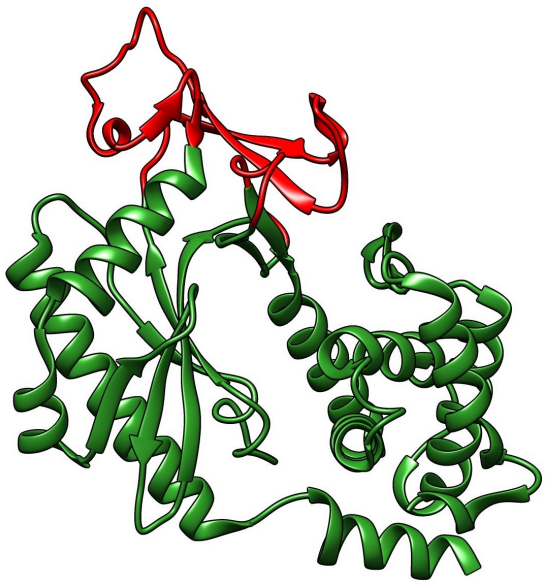

Figure 1.5 : The 3D structure of MiD49 (PDB ID:4woy) visualized in Chimera. Red part is binding site of MiD49

Figure 1.6 : The 3D structure of MiD51 (PDB ID:4nxt) visualized in Chimera. Red part is binding site of MiD51

1.3 Purpose of Thesis

Recent studies have demonstrated that mitochondria are involved in several activities, which are vital for a well-functioning body like calcium homeostasis, programmed cell death, heat production, mitophagy, etc. Mitochondria's dysfunction leads to

chronic diseases. Important symptoms of mitochondrial diseases include diabetes, cancer, Alzheimer, poor growth, heart and kidney diseases. While there have been many molecular docking studies about Drp1-MiD49/51 inhibition recently, Mdivi1 and Dynasore are known inhibitors of mitochondria fission, but they are not suitable for using as drug molecules because of their extensive side effects. As a result, In this study, it was aimed to discover drug candidate molecules with the potential to be a solution against above mentioned diseases and not have side effects like Mdivi1 and Dynasore. During During this study, AutoDock Vina, Ledock and Schrödinger Suite Maestro-Glide XP softwares were used. Moreover, RDKit clustering method was applied on ligands having high docking scores to eliminate similar ligands. Here, a cluster is a collection of small molecules which are divided in groups, based on their molecular fingerprints. Clustering is the process by which the common characteristics of a particular class of compounds are identified. As a result, ligands with similar properties are identified and eliminated so that ligands with different characteristics might be further tested as potential drug candidates and this way we achieve maximum quality in results and future laboratory experiments.

In addition, the study aims to predict pharmaceutical properties of tested ligands by ADME/T calculations so it can be identified whether proposed ligands can be used as possible drugs or not.

Finally, molecular dynamics simulations were performed. MD can be performed using several program packages to simulate protein flexibility and can give us a sight of the possible ways in which top scored inhibitors can behave in a acceptable way when they are bound to their targets and to analyze if docked ligands retain their positions within their respective binding pockets so they can be potentially used as desired inhibitors.

With the combination of different docking calculations, structural, computational and chemical analysis, drug likeness prediction studies and molecular dynamics simulations, this thesis was carried out to screen novel ligands that can be used for mitochondrial fission inhibition.

2. Materials and methods

2.1 Selection of Target Proteins for Molecular Docking Simulations

We took the crystal structures of the target proteins: Nucleotide-free Dynamin 1-like protein (PDB ID: 4BEJ) with resolution 3.48Å visualized in UCSF Chimera in Fig. 1.3, mitochondrial fission protein Drp1 (4WOY) with resolution 2.40Å (Fig. 1.5) and systolic domain of human MiD51 (4NXT) with resolution 2.12Å (Fig. 1.6) from the RCSB PDB and used them for virtual screening and validation using Autodock Vina (referred to as Vina from here on), Ledock and Glide programs against a set of 3.5 million ligands from ZINC database [20]–[26]

2.2 Protein Preparation for Molecular Docking

Our three target proteins and six off-target proteins which were downloaded from RCSB PDB in PDB format was prepared using Protein Preparation Wizard modules of Schrödinger Suite Maestro (Sastry et al., 2013).

2.3 Ligand Preparation for Molecular Docking

Approximately 3.5 million ligands were filtered from approximately 230 million ready-to-dock, purchasable compounds in ZINC Database. The criteria for our selection was their lead-like, 2D In-stock properties (Fig. 2.2). This ligand pack was downloaded as 2D structures in SMILES format. These 3.5 million molecules were converted to 3D structures and after adding hydrogen atoms and deleting non-polar hydrogen atoms prepared as PDBQT file format using OpenBabel for docking calculation [27].

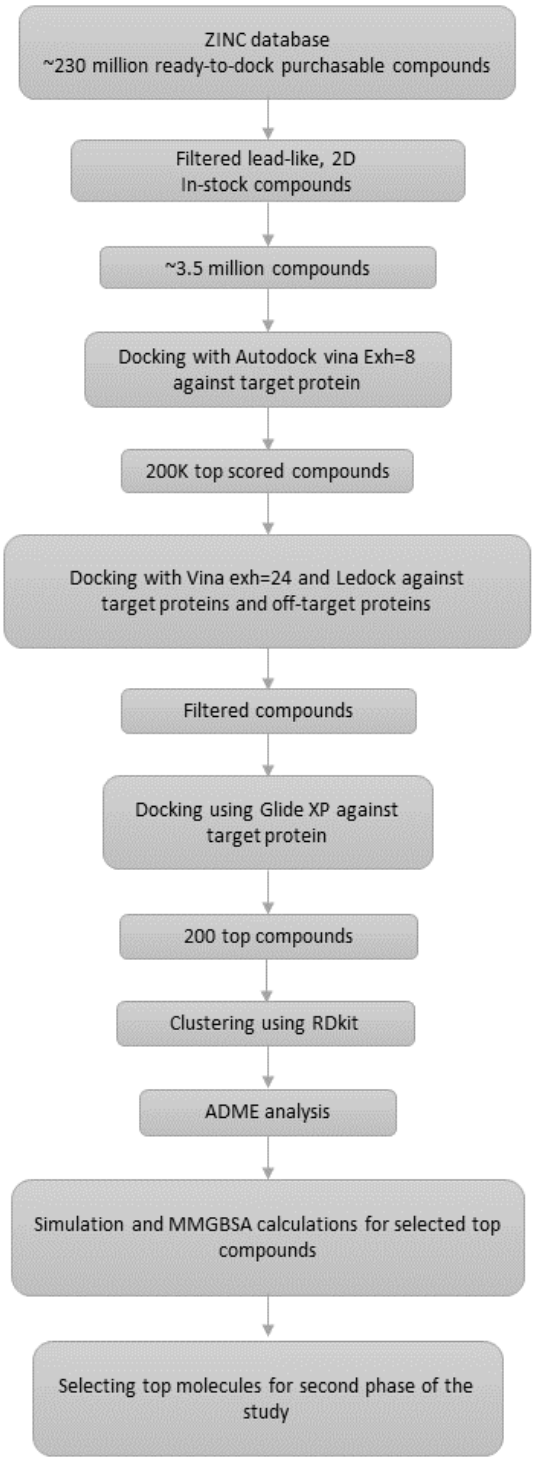

Figure 2.1 : Process flow diagram for docking small molecules against target and off-target proteins and analysis

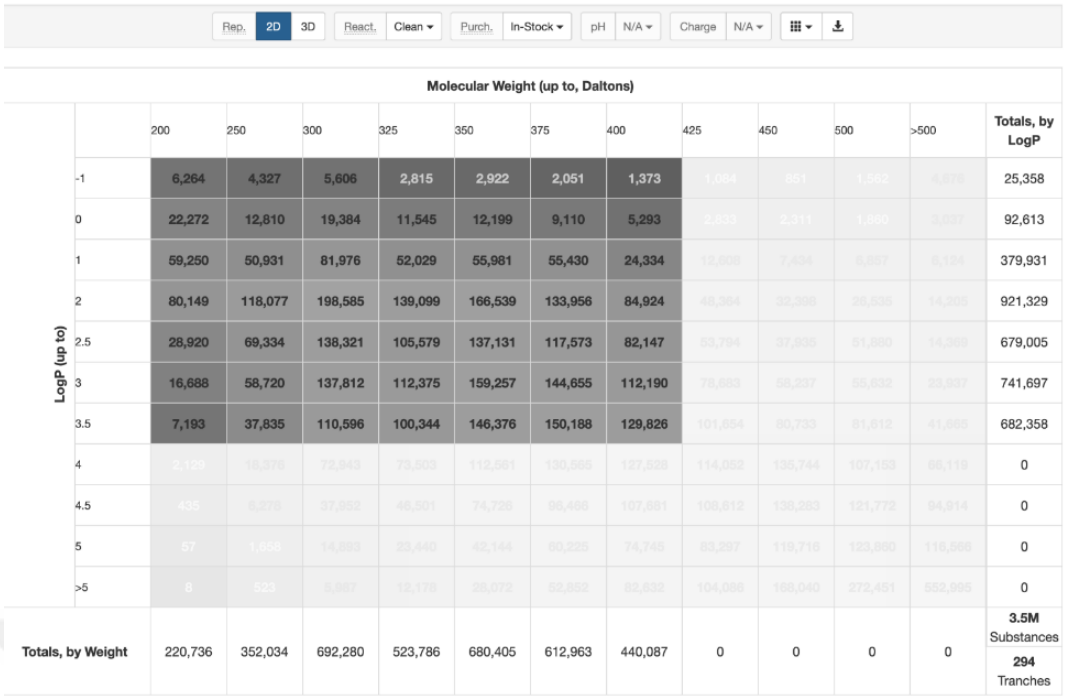

LogP (up to)	200	250	300	325	350	375	400	425	450	500	>500	Totals, by LogP
-1	6,264	4,327	5,606	2,815	2,922	2,051	1,373	1,084	851	1,562	4,679	25,358
0	22,272	12,810	19,384	11,545	12,199	9,110	5,293	2,833	2,311	1,860	3,037	92,613
1	59,250	50,931	81,976	52,029	55,981	55,430	24,334	12,608	7,434	6,897	6,124	379,931
2	80,149	118,077	198,585	139,099	166,539	133,956	84,924	48,364	32,366	28,535	14,205	921,329
2.5	28,920	69,334	138,321	105,579	137,131	117,573	82,147	53,794	37,935	51,880	14,369	679,005
3	16,688	58,720	137,812	112,375	159,257	144,655	112,190	78,883	58,237	55,632	23,937	741,697
3.5	7,193	37,835	110,596	100,344	146,376	150,188	129,826	101,854	80,733	81,612	41,865	682,358
4	2,129	16,376	72,943	73,503	112,561	130,565	127,528	114,052	135,744	107,153	88,119	0
4.5	435	6,378	37,952	46,501	74,726	96,466	107,691	108,812	139,283	121,772	94,914	0
5	57	1,658	14,893	23,440	42,144	60,225	74,745	83,297	119,716	123,860	116,566	0
>5	8	523	5,987	12,178	28,072	52,852	82,632	104,088	168,040	272,451	552,995	0
Totals, by Weight	220,736	352,034	692,280	523,786	680,405	612,963	440,087	0	0	0	0	3.5M Substances 294 Tranches

Figure 2.2 : Selection criteria for small molecules from ZINC database

2.4 Active site of Drp1

According to (kalia,2018) GTP-binding enables Drp1-MiD49/MiD51 interaction. As a result G domain is an important drug binding domain for docking calculations.

2.5 MiD49/51 - Drp1 binding surface

MiD49-Drp1 interacting domain was analyzed using sitemap module of Schrodinger program for the purpose of being a drug binding domain. Sitemap gave us seven potential binding sites and Drp1-MiD49 interaction surface was one of these domains. In this step, designing inhibitors for Drp1-MiD49 and Drp1-MiD51 binding surfaces is planned. MiD49-Drp1 binding surface has high similarity with MiD51-Drp1 binding surface, so inhibition of Drp1 binding to MiD49 and MiD51 seems possible with just one molecule. See Fig. 2.3

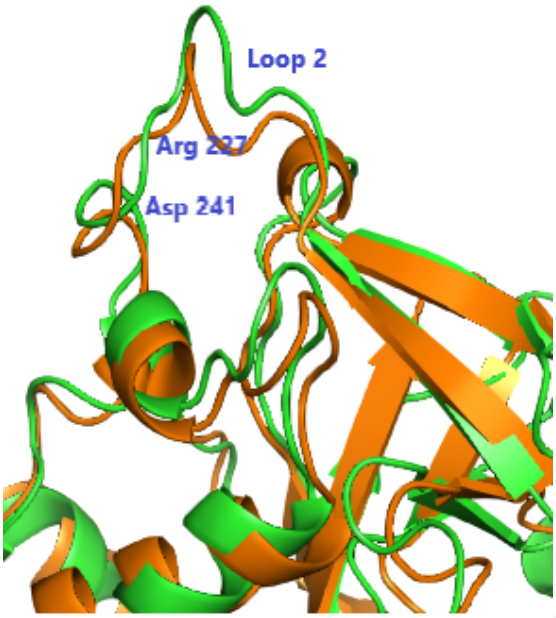

Figure 2.3 : Structural overlay of MiD49 (orange) and MiD51 (green)

2.6 Potential off targets for Drp1-G domain

To make the novel inhibitors more specific for Drp1-Mid49/51 complex, docking calculations for potential off-target proteins was performed too. These inhibitors should have high binding score to our target proteins and at the same time they should have low binding scores when docking into off-target proteins. Proteins having high alignment score with Drp1-G domain have been considered as potential off-targets for designed inhibitors. Proteins with identity score higher than 30% are represented in table 2.1. BLAST method was used for these analysis [28]. 3D structures for these six proteins were extracted from Protein Data Bank. SWISS-Model server was used for modeling missing loops and residues in candidate off-target proteins [29].

Table 2.1 : Off targets for Drp1-G domain

Protein	Uniprot code	Alignment score (%)	PDB ID
Dynamin-1	Q05193	57.1	3SNH
Mx2 protein	P20592	40.6	4WHJ
Mx1 protein	P20591	39.4	4P4U
Mitofusin	Q8IWA4	39.4	5GOE
Rap-2a	P10114	39.2	1KAO
FGFR	O95684	36	4V04

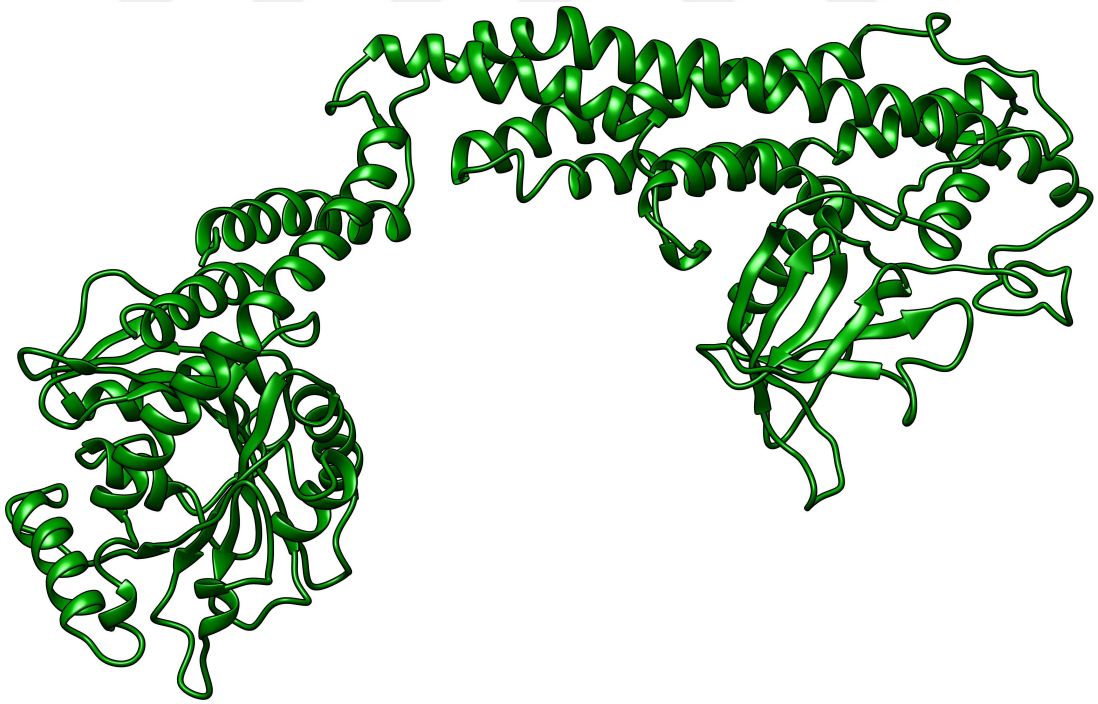

Figure 2.4 : Dynamin1 protein(3SNH)

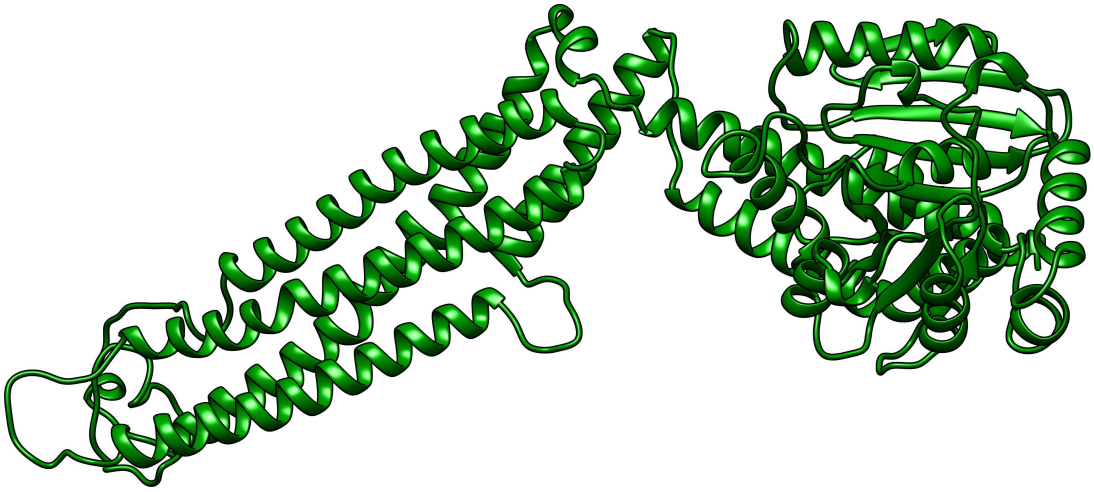

Figure 2.5 : Mx2 Interferon-induced GTP-binding protein (4WHJ)

Figure 2.6 : Mx1 Interferon-induced GTP-binding protein (4P4U)

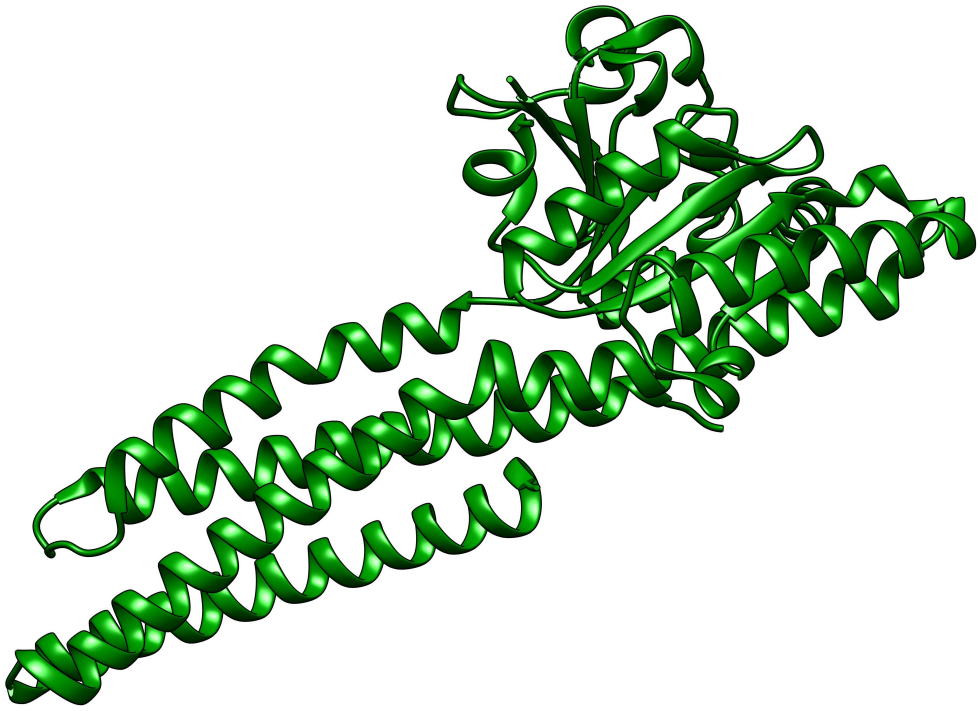

Figure 2.7 : Mitofusin protein (5GOE)

Figure 2.8 : Rap-2a protein (1KAO)

Figure 2.9 : FGFR protein (4V04)

2.7 Potential off targets for MiD49 and MiD51 proteins

MiD49/MiD51-Drp1 binding surface has been selected as the potential drug binding domain, so when searching for off-target proteins, local similarity search was performed instead of using total protein structure. As a result, proteins with local binding domains similar to MiD49/MiD51 proteins binding domains were identified and selected as off-target proteins. In this step, for off-target protein identification five servers have been used: Probis, Ayoubsearch, Dali, RCSB and Yakusa [30]–[34]. One potential protein has been found and used as off-target protein (PDB ID= 5eom).

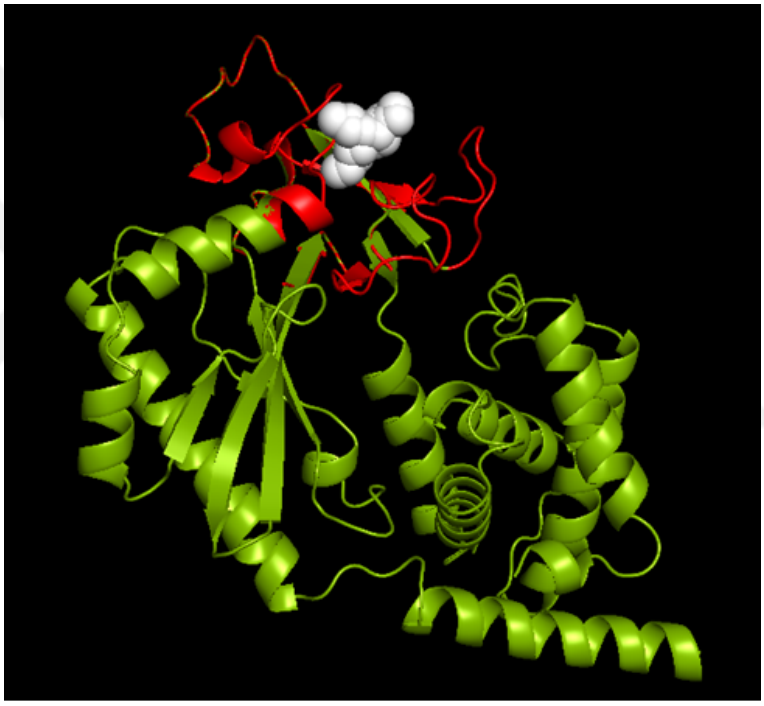

Figure 2.10 : Red: MiD51 (4nxt) protein reduced structure used for off-target search. Green: MiD51 (4nxt). White: Binding domain of MiD51 protein.

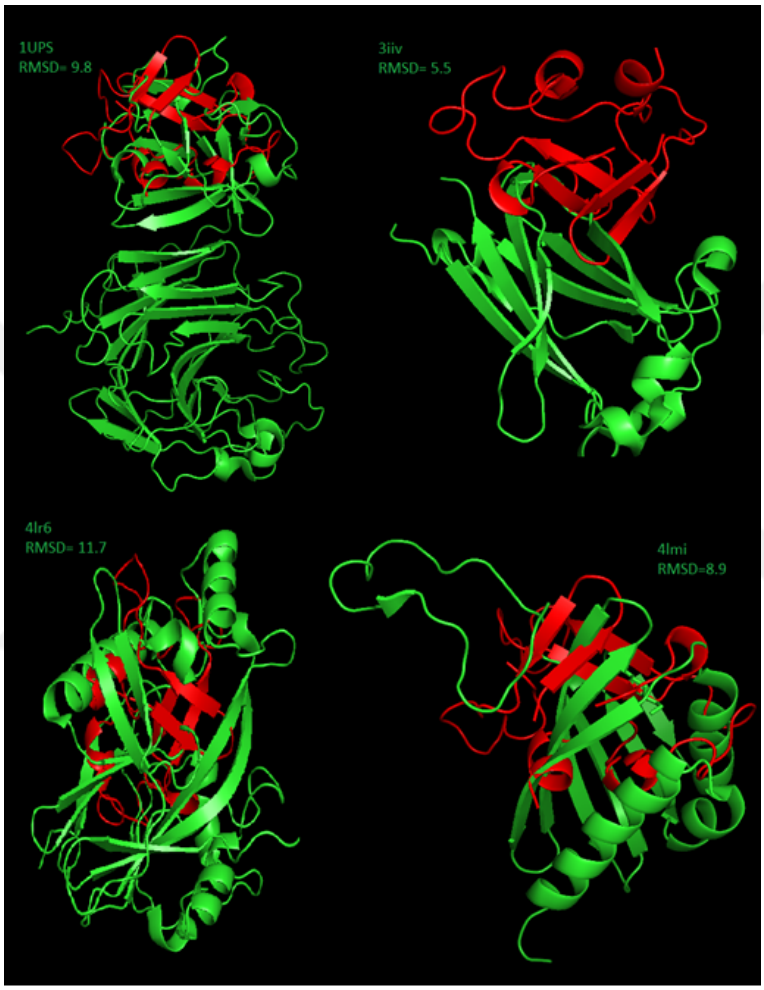

Figure 2.11 : Top scored results for Probis server.

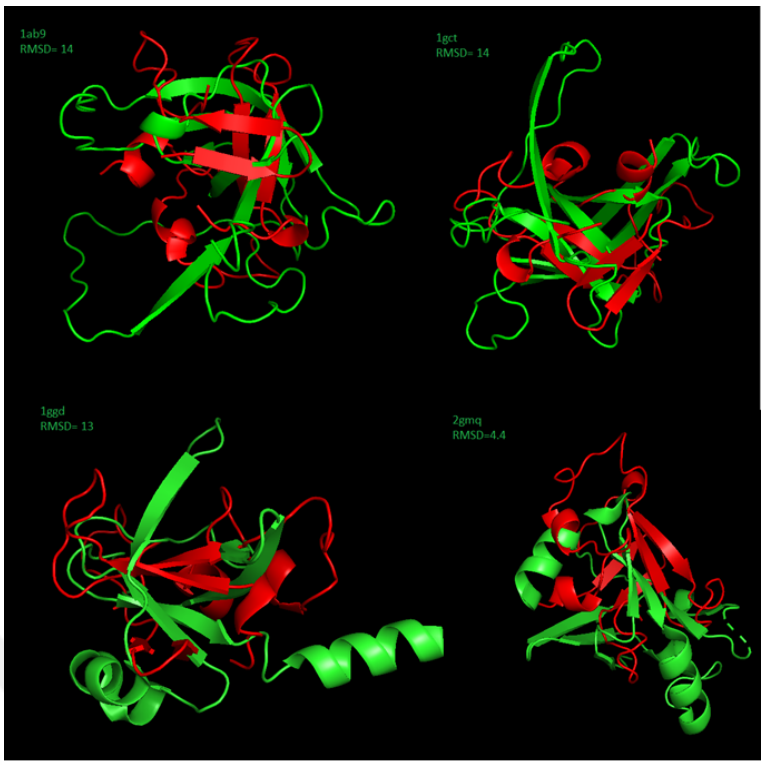

Figure 2.12 : Top scored results for Ayoubsearch server.

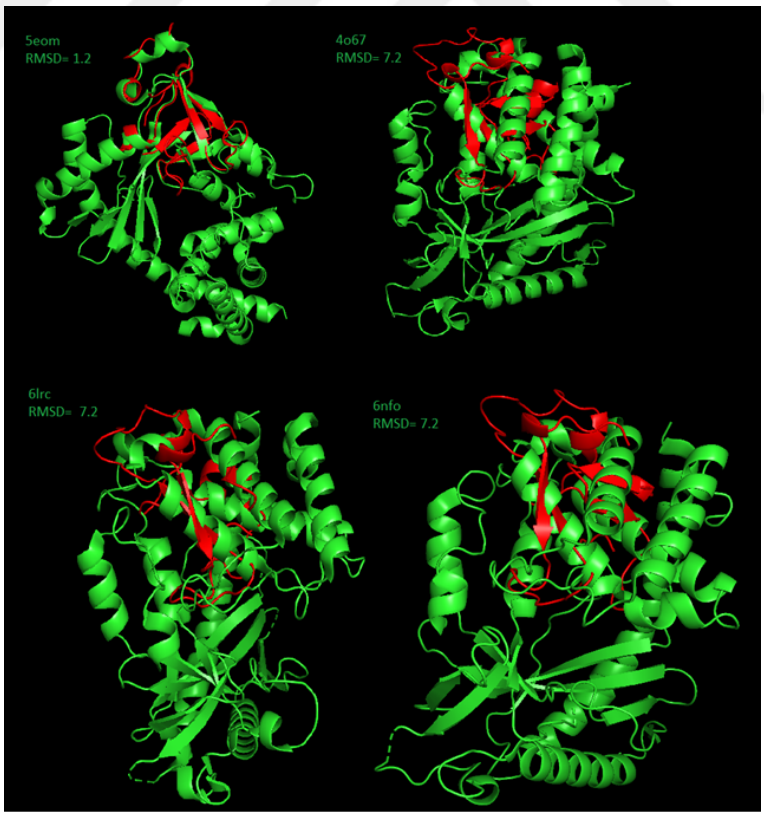

Figure 2.13 : Top scored results for Dali server.

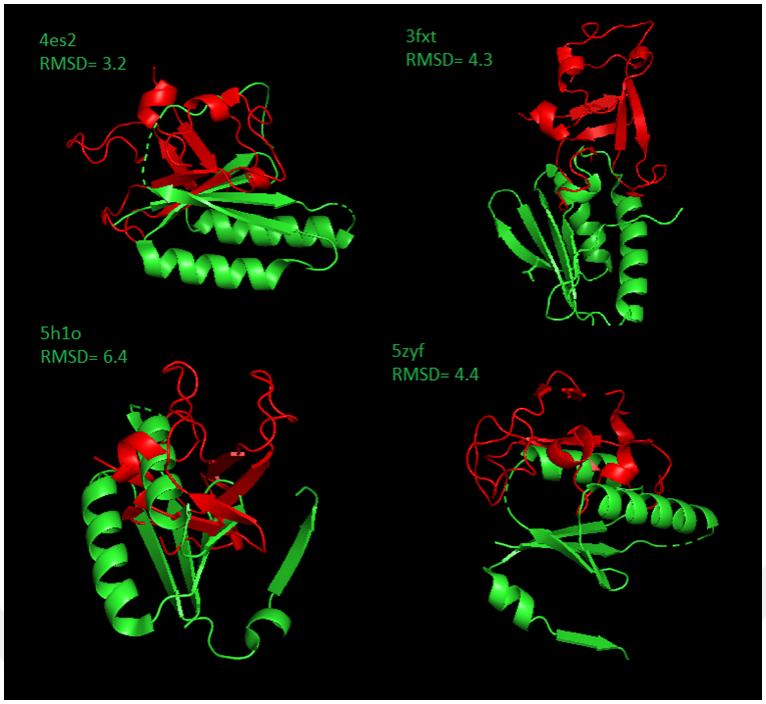

Figure 2.14 : Top scored results for RCSB server.

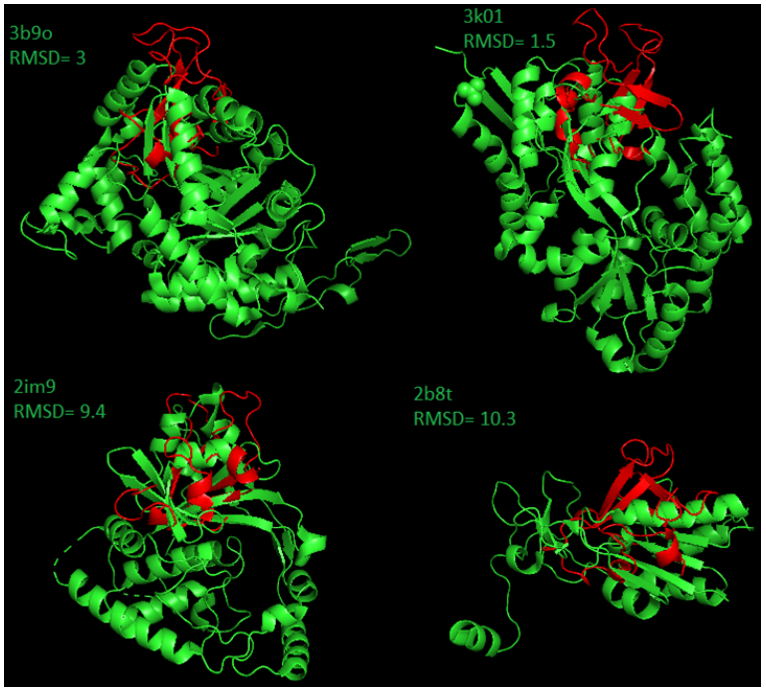

Figure 2.15 : Top scored results for Yakusa server.

2.8 Virtual screening of 3.5 million small molecules against Drp1 proteins

As the first stage of small molecules docking into our target protein Drp1, we performed a molecular docking calculation using Autodock vina program. Here we aimed to screen 3.5 million small molecules which have high binding potential with Drp1. First 200K top scored molecules were filtered to be used in the next step of first packet.

2.9 Virtual screening of 3.5 million small molecules against MiD49/51 proteins

In order to identify molecules that are likely to have the ability to inhibit the binding of MiD49 and MiD51 to Drp1, a second virtual screening for the big set of our data was performed. This approach was taken for docking of 3.5 million molecules from ZINC database into MiD49/MiD51 which are our target receptors in this part. 3D structures for MiD49 and MiD51 taken from PDB are 4woy and 4nxt respectively. 3.5 million molecules docked into MiD49 and MiD51. A collection of 200K top scored molecules was selected for the next step docking calculations. Receptor preparation and other parameters were like previous docking calculation for Drp1-GTPase domain.

2.10 Second stage of screening using Autodock Vina and Ledock programs

A parallel docking calculation was performed for 200K top scored molecules from previous step into our target proteins Drp1 and MiD49/51 proteins using LeDock and AutoDock Vina.

2.11 Extra-precision Docking using Schrödinger Maestro Glide XP for Drp1 protein

Resulted top scored molecules according to our selection criteria (see table 3.1 and 3.2) from previous step were docked into our target protein using Glide extra-precision (XP) docking. Ligprep module of Maestro was used for ligand preparation.

2.12 Clustering analyses using RDKitClusterMolecules module

In this step a clustering analysis was performed. here we aimed to eliminate similar small molecules to avoid performing calculations on molecules with similar activities. Most of the time similar molecules show similar chemical properties so performing analysis on different molecules will help us to achieve a broad range of molecules for the next steps. RDKitClusterMolecules module Clusters molecules based on a variety of 2D fingerprints using Butina or any other available hierarchical clustering methodology and write them to output file(s). We clustered our top scored molecules before ADME/T analysis using this method at a similarity cutoff of 0.55 with automatic determination of number of clusters, and a single SMILES file containing clustered molecules was written along with cluster number for each molecule (2022 Manish Sud.).

2.13 ADME/T analysis using Schrödinger QikProp

ADME/T (Absorption, Distribution, Metabolism, Elimination, and Toxicity) studies, is an important part of drug discovery and development. The prediction of ADME/T properties is critical in the drug design process because these features are responsible for around 60% of all medication failures in clinical trials. In the past, ADME/T tools were used at the end of the drug development process, but today ADME/T is used in the beginning of the process to eliminate compounds with poor ADME/T features from the drug development pipeline, resulting in significant research and development cost and time savings. Absorption is the process in which a chemical substance enters the body. After absorption comes distribution in which the chemical substance or drug moves in the body from one part to another. Third step is metabolism, which refers to converting the initial substance to new compounds. Excretion is required to eliminate compounds and their metabolites from the body. Finally, T stands for toxicity. Selected molecules must have a high biological activity while being non-toxic.

2.14 Molecular Dynamic Simulations using Schrödinger Desmond and MM/GBSA analysis

Previously selected 100 top molecules for our target proteins (Drp1-GTPase, MiD49 and MiD51) were used in molecular dynamic simulation analysis using Schrödinger Desmond. For preparing solvent box for simulation, system builder was used for each protein-ligand complex. Solvent model was set to TIP3P and box shape was orthorhombic, box size calculation method was set to buffer and the system was neutralized by adding needed ions. The system was minimized and solvent system was generated. In the MD simulation step, in molecular dynamics panel of Schrödinger Desmond program, generated solvent system was loaded to workspace, simulation time was set to 100 ns, temperature was set to 300 K. and relax model system before simulation button was checked. results were analyzed by Simulation Interactions Diagram Report panel in Schrödinger Desmond program. In the final step MM/GBSA analysis was performed for 100 top molecules to calculate binding energies of a docked ligand-receptor complex. Molecular mechanics with generalised born and surface area solvation (MM/GBSA) is a popular method to calculate the free energy of the binding of ligands to proteins. It involves molecular dynamics (MD) simulations with an explicit solvent of the protein–ligand complex to give a set of snapshots for which energies are calculated with an implicit solvent. This step was performed for 100 resulted molecules and average and standard deviation was calculated for 30 top scored molecules. The results are represented in table 3.3.

3. Results

3.1 Virtual screening for nearly 3.5 million molecules against Drp1 protein

Before docking calculations, a molecular similarity measurment using RDkit python library was performed to eliminate similar molecules to Mdivi and Dynasore [35]. As a result 33 molecules had 70% and above similarity with Mdivi-1 and no similar molecules were identified for Dynasore. These 33 molecules have been removed from the list of ready to dock molecules for the next step. This approach was taken for the novel inhibitors in order not to have unwanted side-effects of Mdivi and Dynasore.

In this step DRP1 (4bej) was used as our target protein and a docking calculation was performed for 4bej and 3.5 million small molecules from ZINC database. Vina program was used for preliminary screening of 3.5 million molecules. A collection of 200K with lowest binding affinity was selected for further computations. For Vina calculations, the receptor and small molecules format converted to the PDBQT format using open babel [36]. Grid box coordinates used in Vina was set to (38.59 , 68.13, -103.94), grid box size was set to 30*30*30 and exhustiveness parameter was set to 8 in this step. Fig. 3.1 shows docking results distribution.

3.2 Virtual screening of 200K top molecules from previous step using Ledock and Autodock Vina with exhaustiveness 24

In this step, 200K top scored molecules from previous step were selected for docking into DRP1 (4BEJ) again using different programs. Binding energies for selected 200K top molecules were between -9.9 and -8.4 kcal/mol. Virtual screening for 200K top molecules was performed using Vina and LeDock programs. The exhaustiveness parameter for Vina was set to 24. For LeDock, RMSD parameter was setted to 1Å. Results are represented in Figs. 3.2 and 3.3 [4].

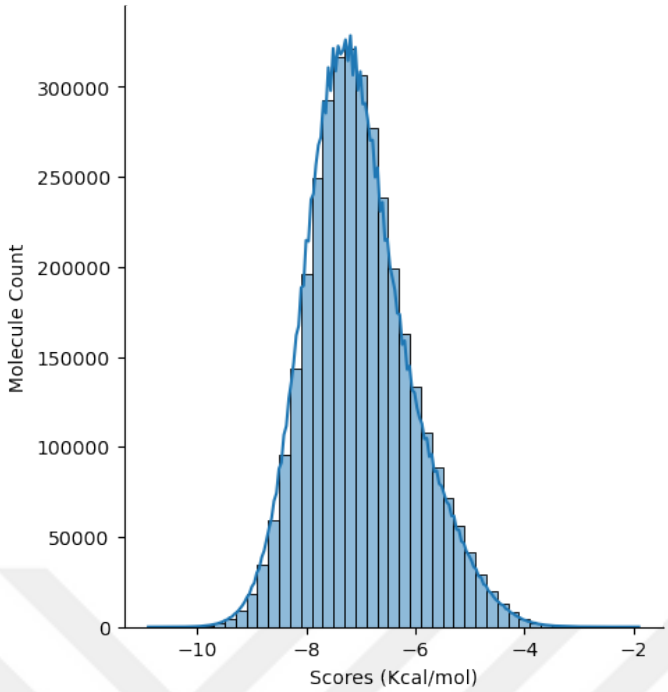

Figure 3.1 : Distribution of docking scores for 3.5 million molecules and DRP1-GTPase using Vina

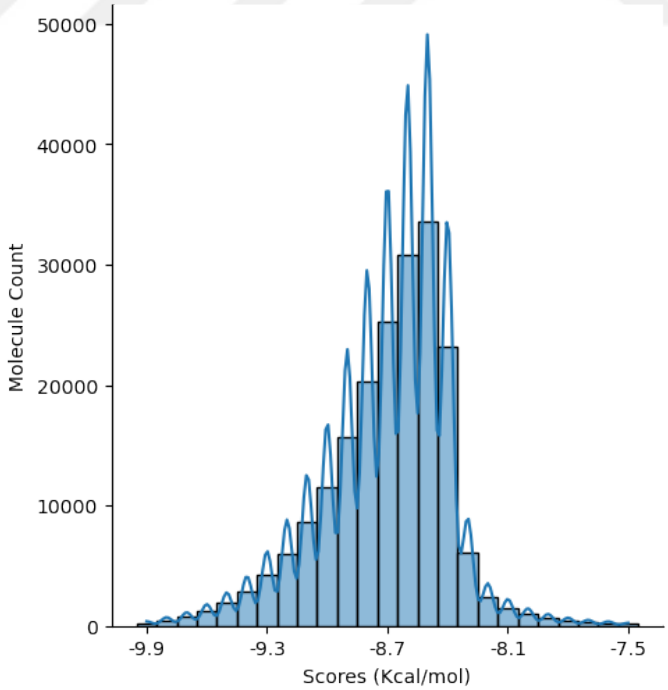

Figure 3.2 : Distribution of docking scores for 200K top-scored molecules and DRP1-GTPase using Autodock Vina

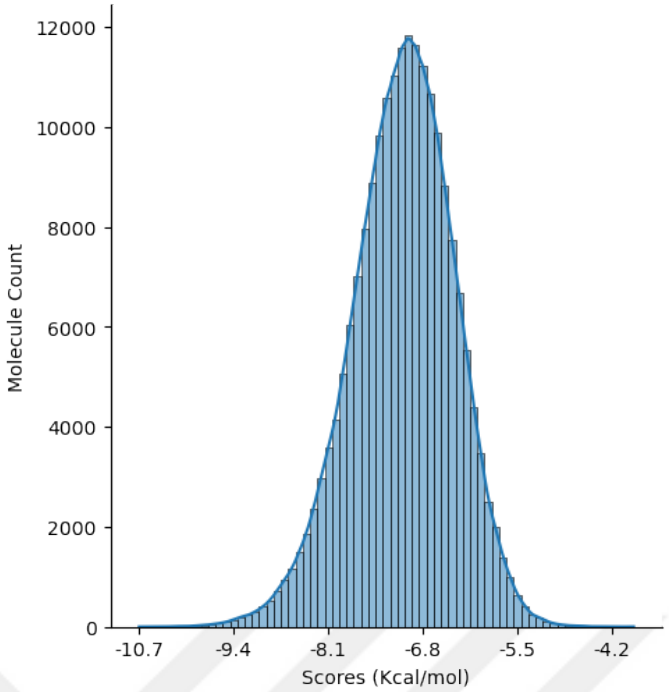

Figure 3.3 : Distribution of docking scores for 200K top-scored molecules and DRP1-GTPase using Ledock

3.3 Off-target proteins docking calculations with Ledock and AutoDock Vina

A docking calculation was performed for 200K top scored molecules from previous step into six Off-target proteins of DRP1-GTPaz domain using LeDock and AutoDock Vina. The representation of the distribution graphs for Vina and Ledock results are in Figs. 3.4 and 3.5.

3.4 Extra precision Docking with Glide XP

First we wanted to perform a docking calculation on common small molecules which were in 5000 first top scored molecules bound to our target protein (DRP1-GTPaz) and in 10000 low scored molecules which bound to Off-target proteins using Vina and Ledock. This approach did not give us a good result and enough molecules to perform docking calculation using Glide XP program. So we changed our criteria for selecting molecules for the next step. Molecules with binding scores smaller than -9.5 kcal/mol for DRP1-GTPase protein with Vina and molecules with binding scores bigger than -8.5 kcal/mol for off-target proteins which their count is 318, were selected

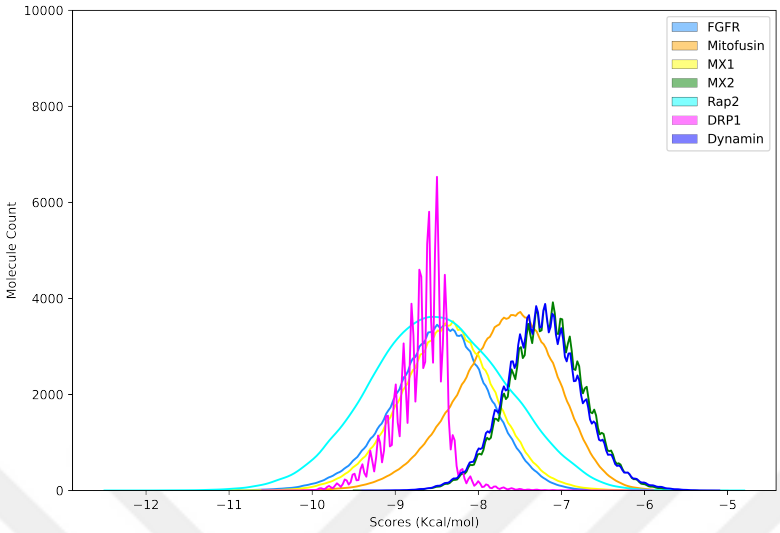

Figure 3.4 : Six Off Targets distribution graph-Vina

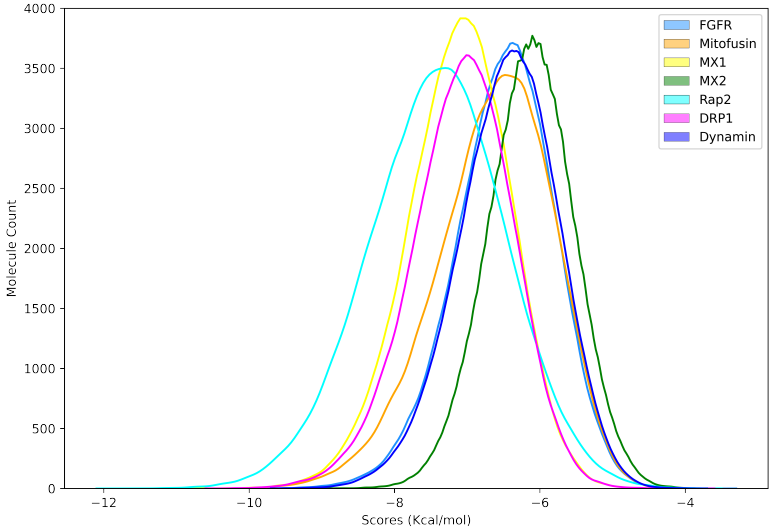

Figure 3.5 : Six Off Targets distribution graph-Ledock

to perform further docking calculations, and at the same time, molecules with binding score smaller than -8.5 kcal/mol and bigger than -8 kcal/mol for DRP1-GTPase protein using LeDock program which their count is 448 in total 766 molecules were selected for docking calculations with Glide XP. The strategy in this step helps us identify molecules with high binding affinity to target protein and at the same time low binding affinity to off-target protein. A docking step was performed for resulted molecules from this step using Schrodinger program Glide (XP docking) module. 200 high scored molecules from this step were selected for the next step. Distribution graph for docking scores is shown in Fig. 3.6.

Table 3.1 : Selection criteria for Vina results

Drp1-GTPaz	Off-Target proteins	Molecule count
<= -10	>= -8.5	8
<= -9.5	>= -8.5	318
<= -10	>= -9	69

Table 3.2 : Selection criteria for Ledock results

Drp1-GTPaz	Off-Target proteins	Molecule count
<= -9	>= -8	59
<= -8.5	>= -8	448
<= -8.8	>= -8	127

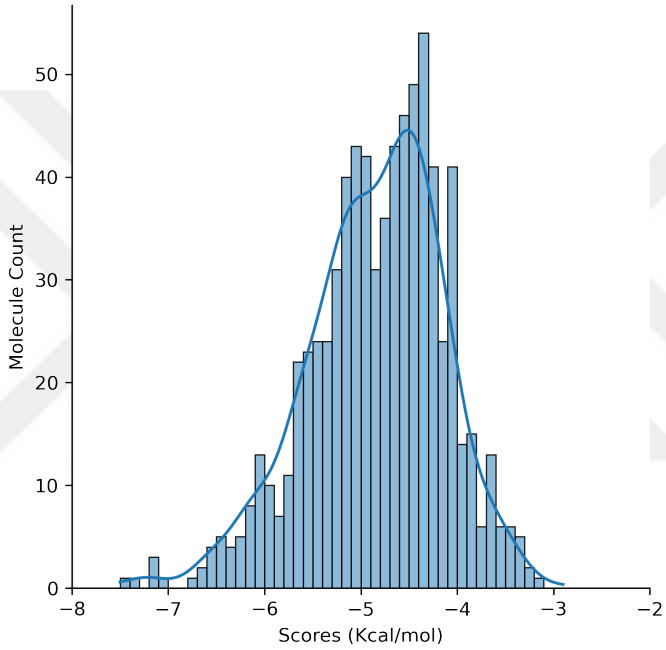

Figure 3.6 : Distribution of binding scores of 766 molecules docked to DRP-GTPaz domain using Glide XP

3.5 Clustering and ADME analysis

According to binding results, 200 top scored molecules were selected to perform a clustering analysis on. Clustering analysis was performed using RDKit clustering algorithm. This algorithm gave us 165 clusters and one cluster centroid were identified from each cluster for further steps. ADME/T analysis were performed for these 165 representative molecules using Schrodinger QuikProp module, and 100 top scored molecules were identified.

3.6 MD Simulation and MMGBSA calculations and identifying molecules to be experimentally tested

In this step, a 100 ns MD simulation have been performed and a MMGBSA calculation was performed to calculate the free energy of binding for 100 molecules from previuos step and average and standard deviation was calculated for 30 top scored molecules. The results are represented in table 3.3.

3.7 Virtual screening of 3.5 million molecules and MiD49/51 proteins

3.5 million molecules docked into MiD49 and MiD51. A collection of 200K top scored molecules had been selected for the next step docking calculations. Receptor preparation and other parameters were like previous docking calculation for DRP1-GTPase domain. Binding scores distribution graphs are represented in Figs. 3.7 and 3.8

3.8 Virtual screening of 200K top scored molecules from previous step

Here 200K top scored molecules had been docked into MiD49 and MiD51 again using Vina with exhusstiveness of 24 and Ledock programs. Binding scores distribution graphs are represented in Figs. 3.9 , 3.10, 3.11 and 3.12

Table 3.3 : MMGBSA results for 30 top scored molecules

NO	ZINC ID	Average	Standard deviation
1	ZINC000001140543	-110,14	8,34
2	ZINC000253537615	-100,49	6,11
3	ZINC001547200808	-99,97	10,92
4	ZINC000067946823	-92,93	4,72
5	ZINC000952980688	-92,75	10,12
6	ZINC000005059006	-91,81	4,96
7	ZINC000013719692	-88,42	11,73
8	ZINC000067713967	-86,70	6,15
9	ZINC000070655646	-86,02	4,83
10	ZINC000038828716	-85,33	6,05
11	ZINC000004741865	-82,88	5,57
12	ZINC000091410801	-82,52	4,62
13	ZINC000020719341	-82,11	5,13
14	ZINC000019499138	-81,92	7,16
15	ZINC000072142105	-81,91	6,32
16	ZINC000019579107	-81,80	5,74
17	ZINC000011935387	-81,58	7,10
18	ZINC000032092058	-81,42	4,73
19	ZINC000067713443	-81,42	6,38
20	ZINC000091587449	-80,40	5,98
21	ZINC000575414329	-79,90	7,97
22	ZINC000055370420	-79,29	4,96
23	ZINC000004880668	-79,15	5,55
24	ZINC000090558863	-78,96	5,20
25	ZINC000019220340	-78,96	4,30
26	ZINC000096149474	-78,92	11,56
27	ZINC000014981763	-78,38	5,93
28	ZINC000408586602	-78,13	4,56
29	ZINC000007980469	-78,01	4,36
30	ZINC000224262106	-77,76	7,24

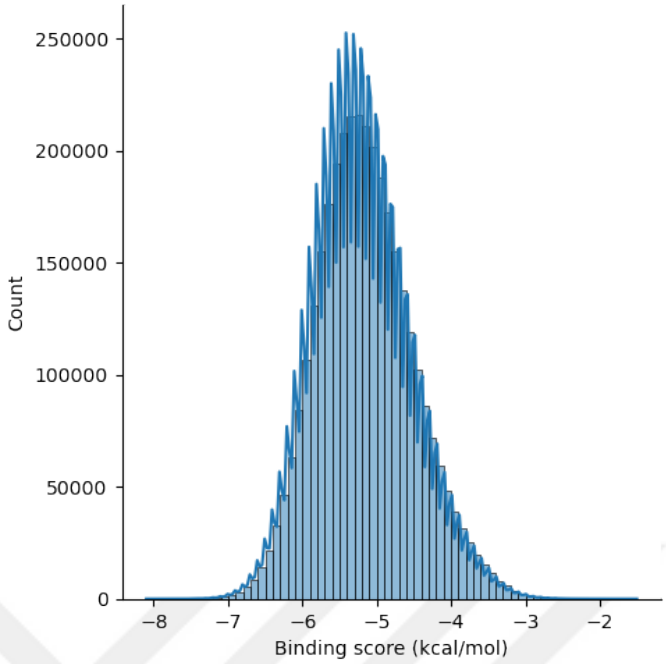

Figure 3.7 : Binding scores distribution graph for 3.5 million small molecules and MiD51 protein

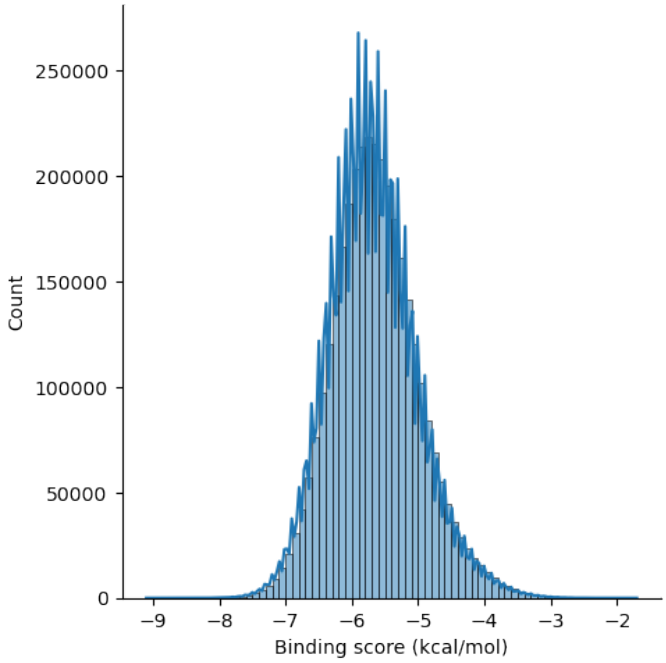

Figure 3.8 : Binding scores distribution graph for 3.5 million and MiD49 protein

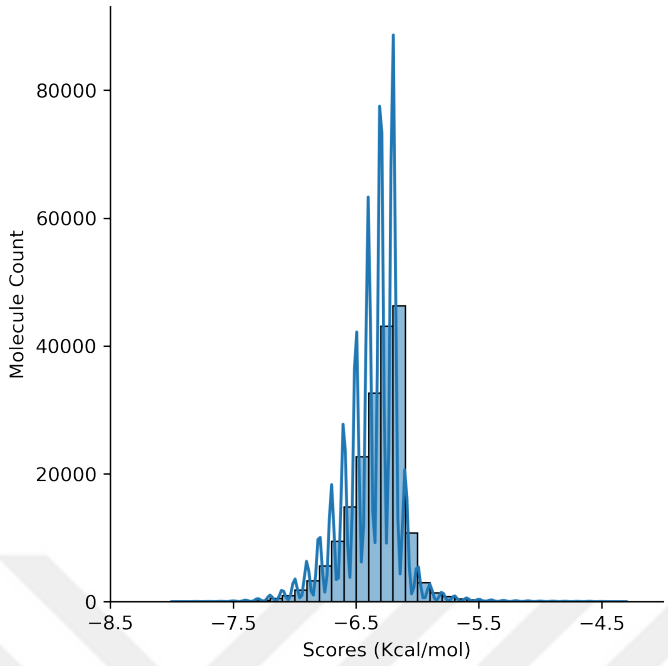

Figure 3.9 : Distribution of docking scores for 200K top-scored molecules and MiD51 (4nxt) using Autodock Vina

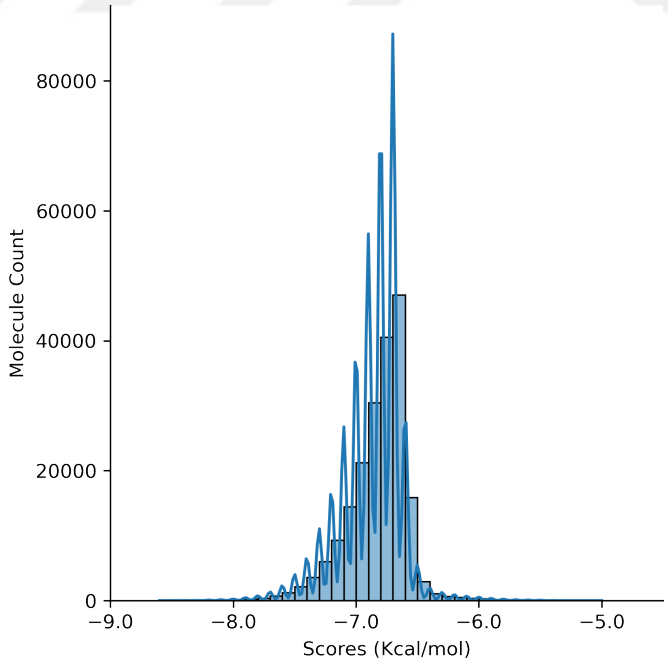

Figure 3.10 : Distribution of docking scores for 200K top-scored molecules and MiD49 (4woy) using Autodock Vina

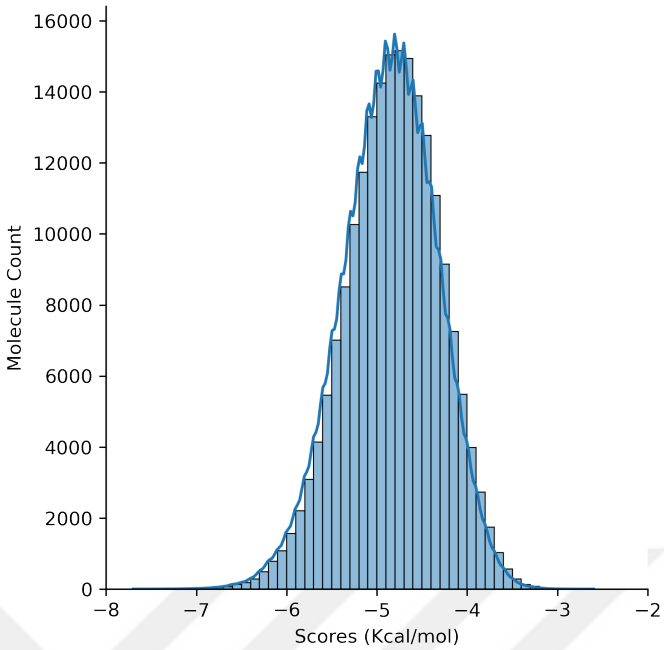

Figure 3.11 : Distribution of docking scores for 200K top-scored molecules and MiD51 (4nxt) using Ledock

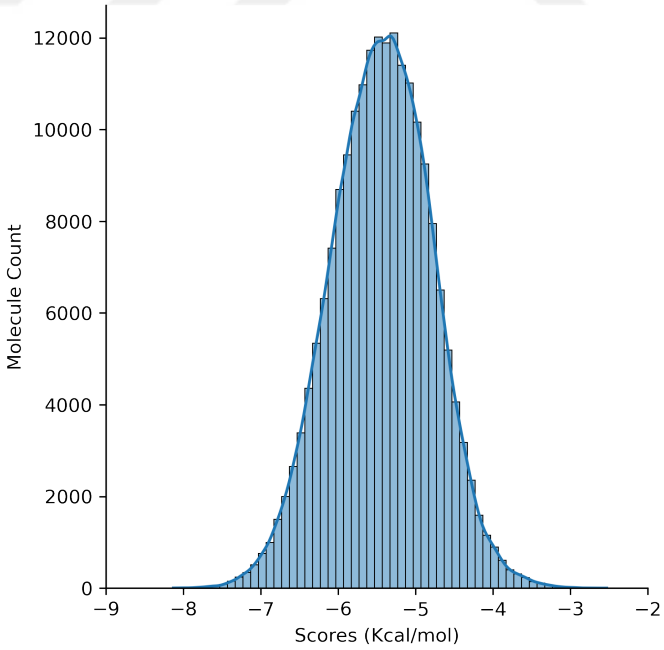

Figure 3.12 : Distribution of docking scores for 200K top-scored molecules and MiD49 (4woy) using Ledock

3.9 Off-target proteins docking calculations for MiD49 and MiD51 using Ledock and AutoDock Vina

A docking calculation was performed for 200K top scored molecules from previous step into one Off-target protein of MiD49/51 using LeDock and AutoDock Vina. The representation of the distribution graphs for Vina and Ledock results are in Figs. 3.13 and 3.14

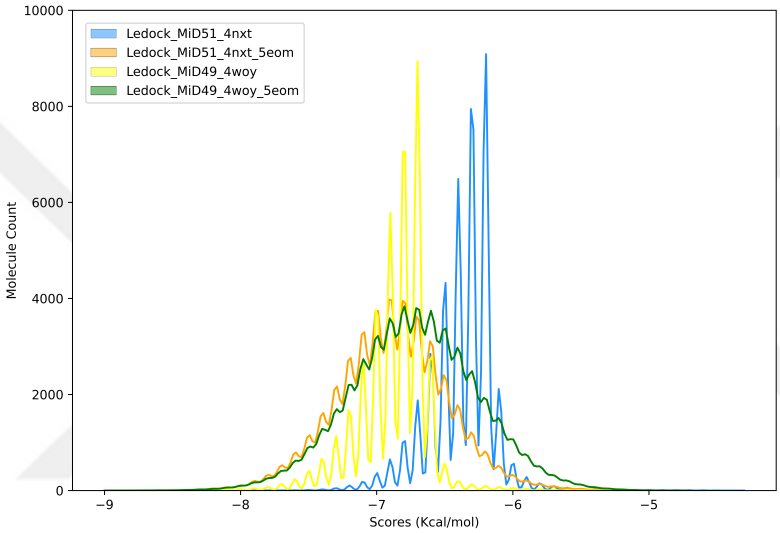

Figure 3.13 : Distribution of docking scores for 200K top-scored molecules and off-target protein (5eom) of MiD49/51 using Vina

3.10 Extra precision Docking with Glide XP

In this part we used a different approach for selecting candidate molecules for docking using Glide XP. In vina results, we selected 899 common molecules from results of docking calculations which its selection criteria is represented in table 3.4.

In Ledock results, we selected 169 common molecules from results of docking calculations which its selection criteria is represented in table 3.5

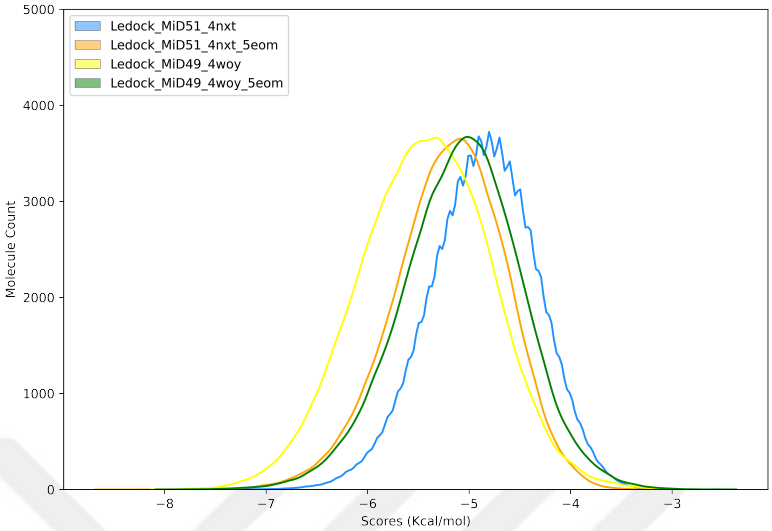

Figure 3.14 : Distribution of docking scores for 200K top-scored molecules and off-target protein (5eom) of MiD49/51 using Ledock

Table 3.4 : Selection criteria for Vina results

4nxt and 4woy	Off-Target protein(5eom)	Common molecule count
First 5K	Last 10K	0
First 50K	Last 30K	53
First 50K	Last 50K	170
First 50K	Last 80K	502
First 50K	Last 100K	899
First 80K	Last 100K	2396
First 100K	Last 50K	746

Table 3.5 : Selection criteria for Ledock results

4nxt and 4woy	Off-Target protein(5eom)	Common molecule count
First 5K	Last 10K	0
First 50K	Last 30K	0
First 50K	Last 50K	3
First 50K	Last 80K	49
First 50K	Last 100K	169
First 80K	Last 100K	887
First 100K	Last 50K	100

In total 1068 molecules were selected for docking calculations using Glide XP. The strategy in this step helps us identify molecules with high binding affinity to target protein and at the same time low binding affinity to off-target protein. A docking calculation was performed for resulted molecules from this step using Schrodinger program Glide (XP docking) module. Distribution graph for docking scores is shown in Fig. 3.15.

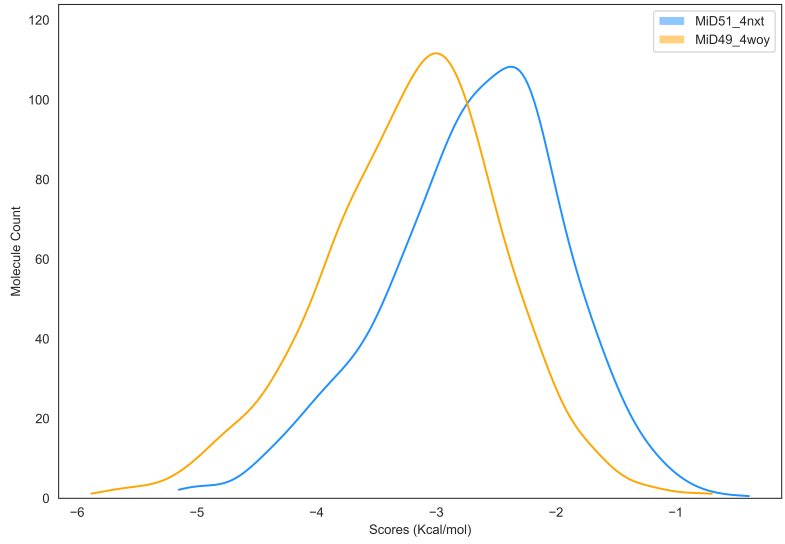

Figure 3.15 : Distribution of docking scores using Glide XP for MiD51 (4nxt) represented in blue and MiD49 (4woy) represented in orange using Glide XP

3.11 Clustering and ADME/T analysis

From previous step, among 200 top scored molecules of MiD49 and MiD51 results 59 common molecules were selected to perform a clustering analysis on. Clustering analysis was performed using RDKit clustering algorithm. This algorithm gave us 52 clusters and one cluster centroid were identified from each cluster for further steps. ADME/T analysis were performed for these 52 representative molecules using Schrodinger QuikProp module, and 31 top scored molecules which were ready to purchase were identified.

3.12 Molecular Dynamics Simulations identifying molecules to be experimentally tested

In this step, a 100 ns MD simulation have been performed. Root mean square deviation (RMSD) and ligand-protein interaction analyses using Desmond simulation interactions diagram were performed for ten randomly selected ligand-receptor structures among 30 high scored compounds of MiD49 and MiD51 proteins. Results are shown in below figures.

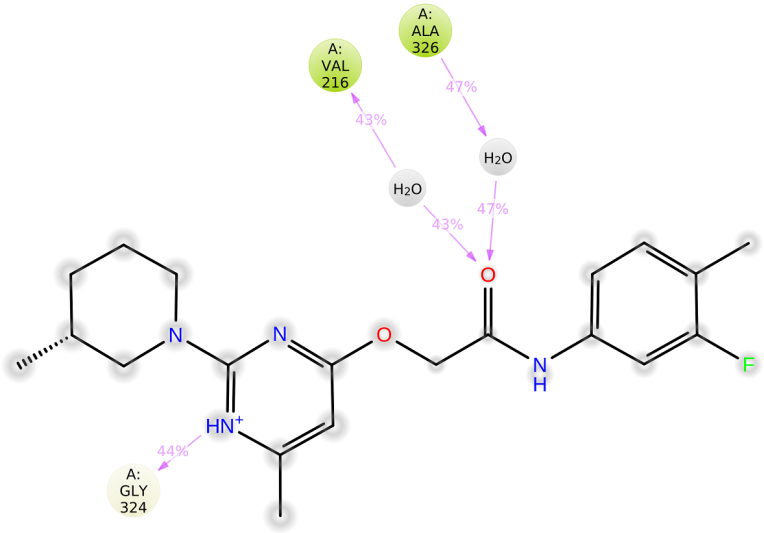

(a)

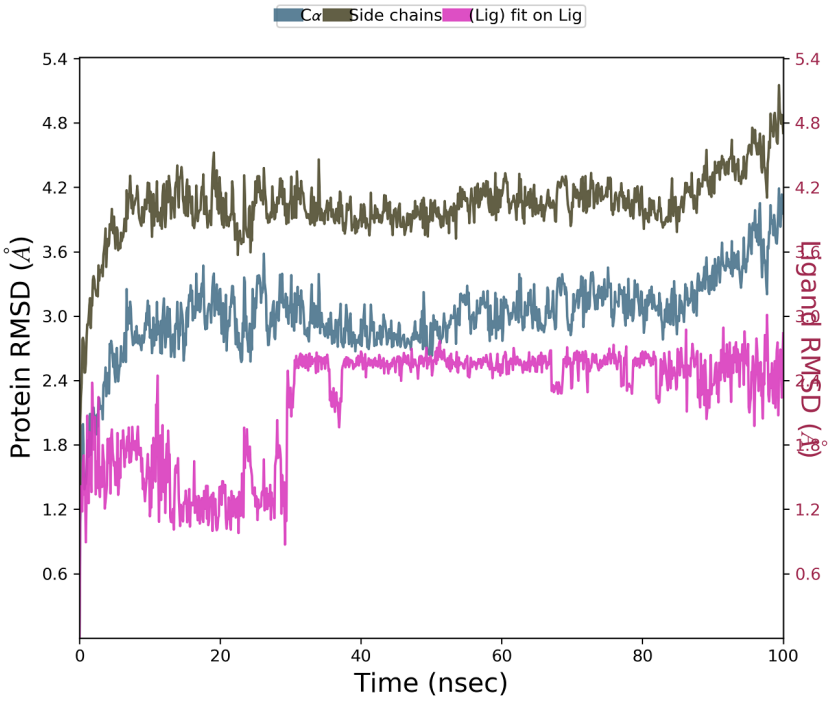

(b)

Figure 3.16 : The schematic of a) detailed ligand atom (ZINC000091914856) interactions with the protein residues. Red residue: Negatively charged, Purple residue: Positively charged, White residue: Glycine, Yellow residue: Hydrophobic, Blue residue: Polar, Purple arrow: H-bond, Orange arrow: Halogen Bond, Purple line: Metal coordination, Green line: Pi-Pi stacking, Grey circle: Solvent exposure.and b) Protein-Ligand RMSD analyses of ZINC000044168468 with MiD49 receptor, using Schrödinger Meastro simulation interactions diagram.

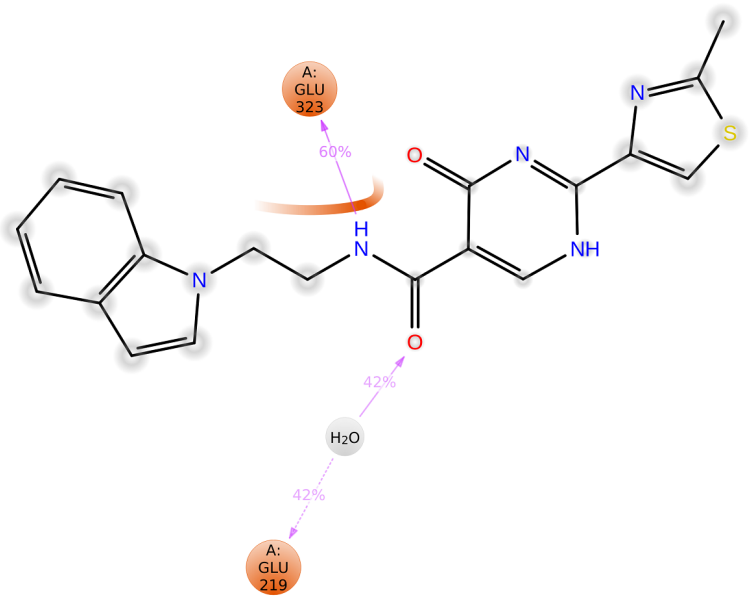

(a)

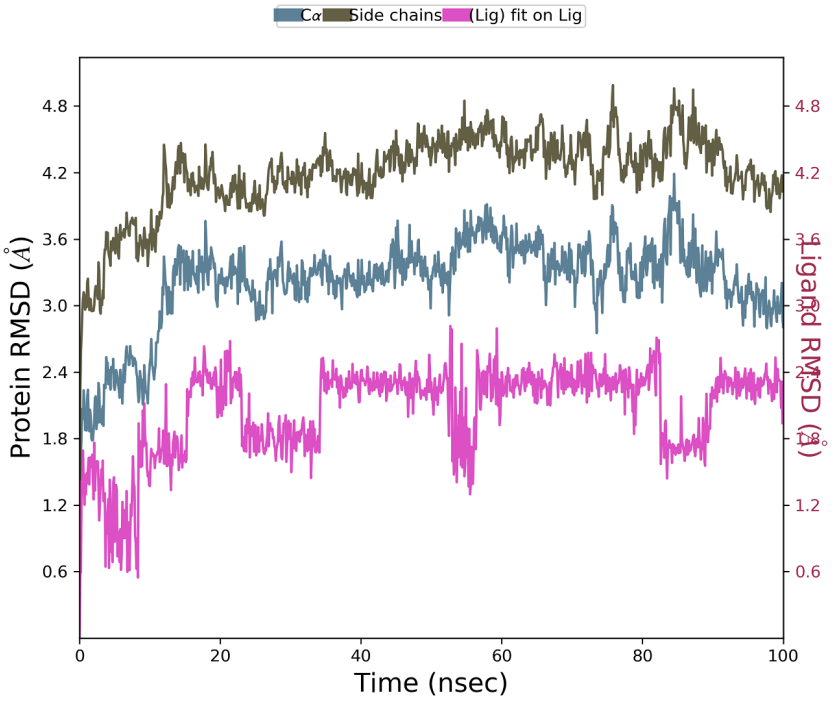

(b)

Figure 3.17 : The schematic of a) detailed ligand atom (ZINC000091914856) interactions with the protein residues. Red residue: Negatively charged, Purple residue: Positively charged, White residue: Glycine, Yellow residue: Hydrophobic, Blue residue: Polar, Purple arrow: H-bond, Orange arrow: Halogen Bond, Purple line: Metal coordination, Green line: Pi-Pi stacking, Grey circle: Solvent exposure.and b) Protein-Ligand RMSD analyses of ZINC000091914856 with MiD49 receptor, using Schrödinger Meastro simulation interactions diagram.

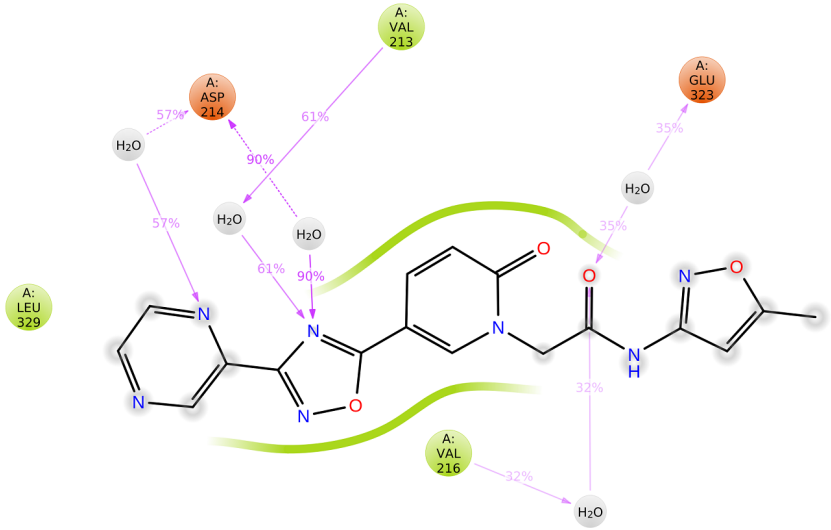

(a)

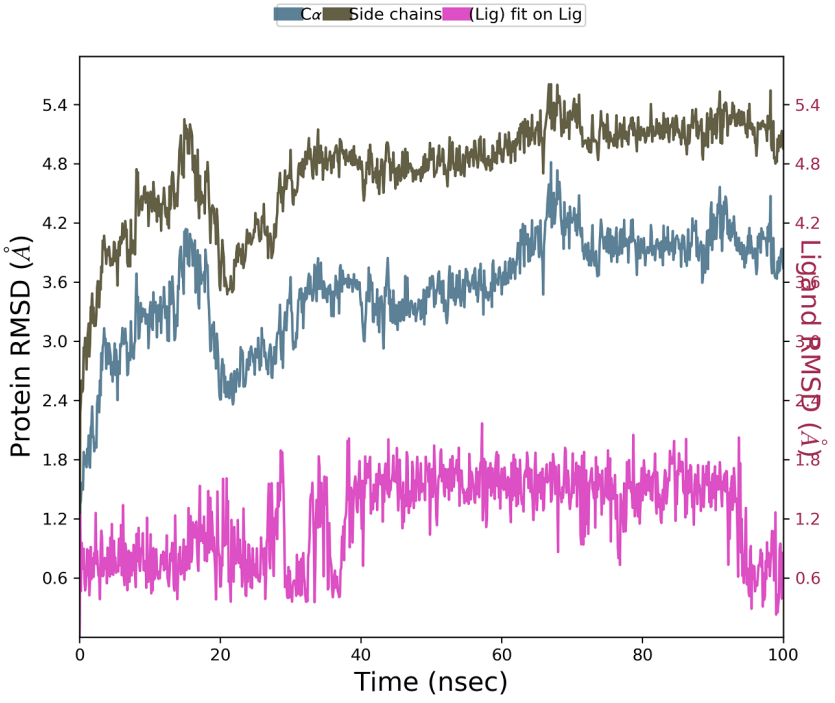

(b)

Figure 3.18 : The schematic of a) detailed ligand atom interactions with the protein residues. Red residue: Negatively charged, Green residue: Hydrophobic, Purple arrow: H-bond, Green line: Pi-Pi stacking, Grey circle: Solvent exposure. b) Protein-Ligand RMSD analyses of ZINC000077199968 with MiD49 receptor, using Schrödinger Meastro simulation interactions diagram.

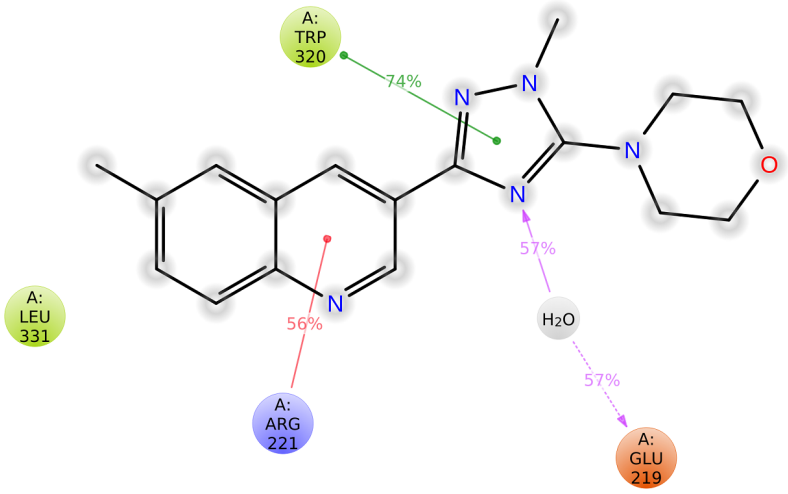

(a)

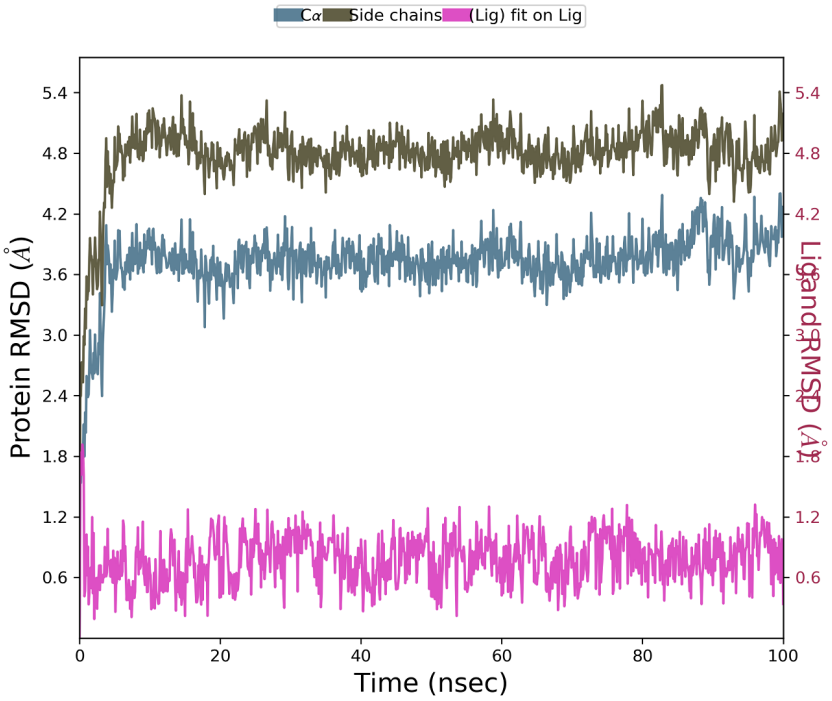

(b)

Figure 3.19 : The schematic of a) detailed ligand atom interactions with the protein residues. Red residue: Negatively charged, Purple residue: Positively charged, White residue: Glycine, Yellow residue: Hydrophobic, Blue residue: Polar, Purple arrow: H-bond, Orange arrow: Halogen Bond, Purple line: Metal coordination, Green line: Pi-Pi stacking, Grey circle: Solvent exposure.and b) Protein-Ligand RMSD analyses of ZINC000426430637 with MiD49 receptor, using Schrödinger Meastro simulation interactions diagram.

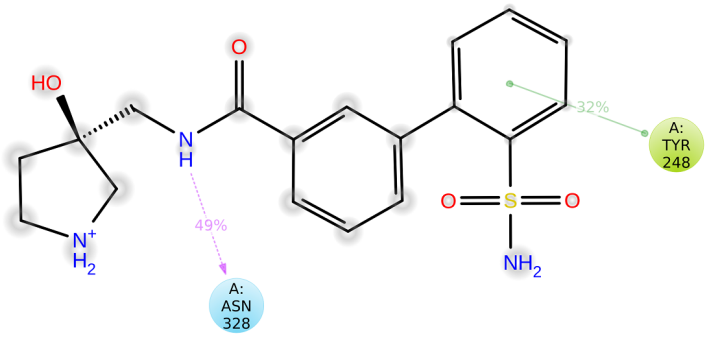

(a)

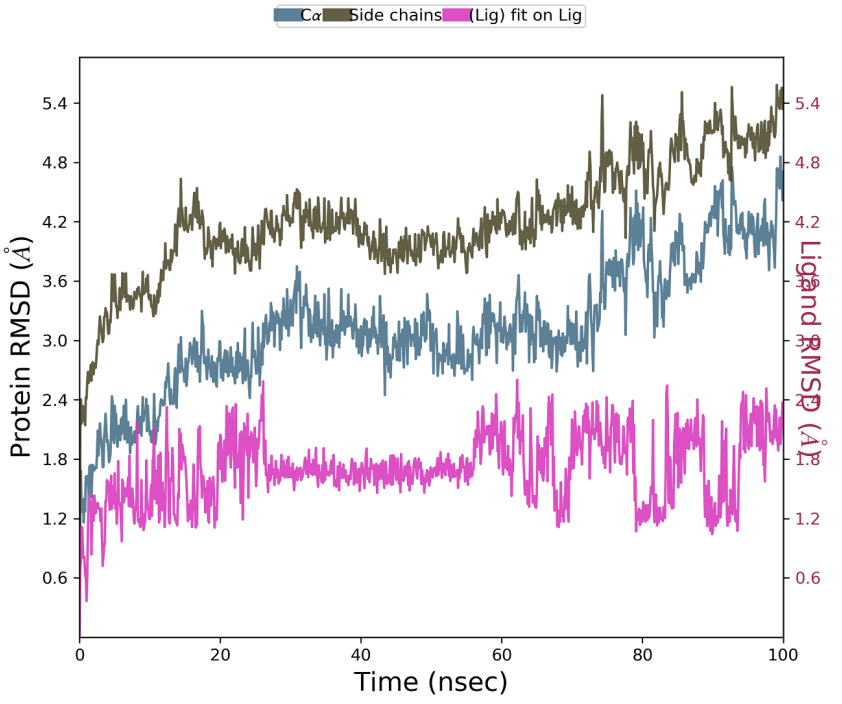

(b)

Figure 3.20 : The schematic of a) detailed ligand atom interactions with the protein residues. Red residue: Negatively charged, Purple residue: Positively charged, White residue: Glycine, Yellow residue: Hydrophobic, Blue residue: Polar, Purple arrow: H-bond, Orange arrow: Halogen Bond, Purple line: Metal coordination, Green line: Pi-Pi stacking, Grey circle: Solvent exposure.and b) Protein-Ligand RMSD analyses of ZINC000426379642 with MiD49 receptor, using Schrödinger Meastro simulation interactions diagram.

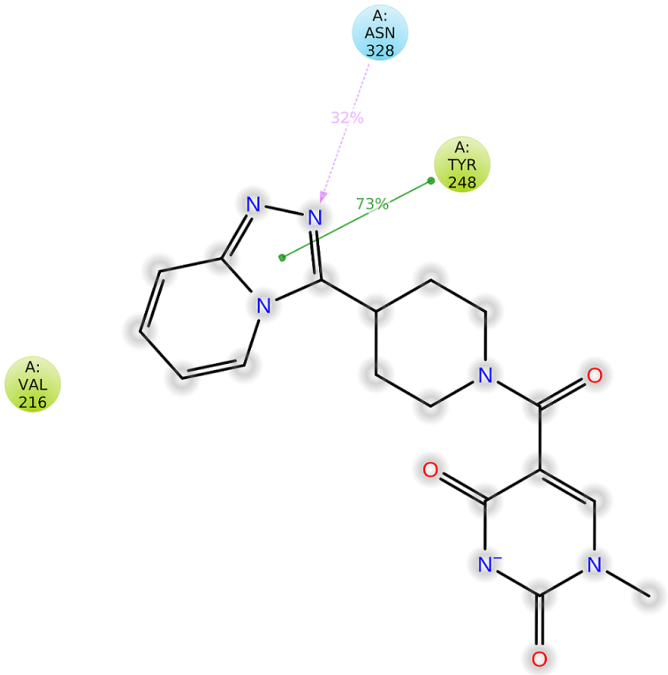

(a)

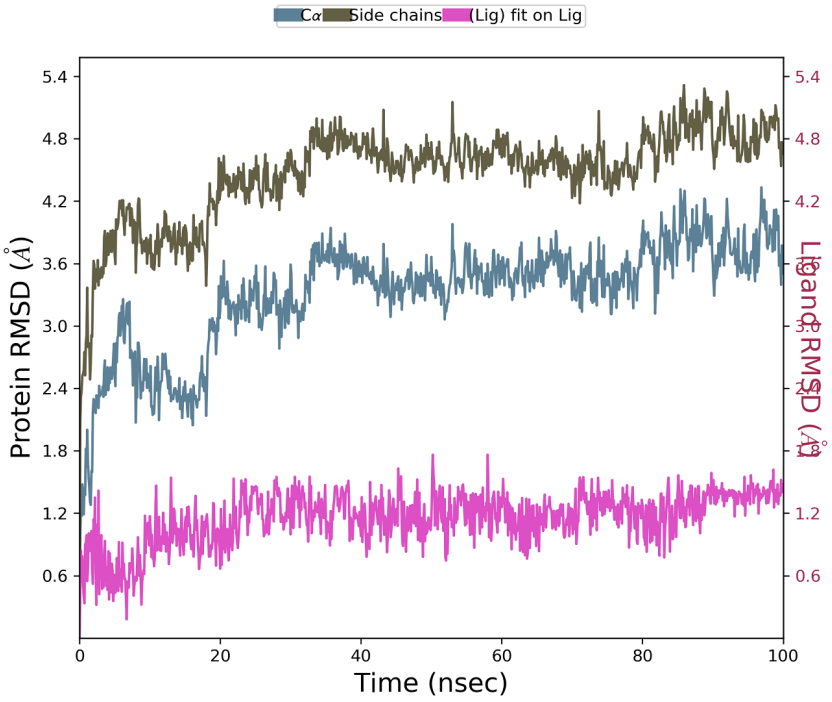

(b)

Figure 3.21 : The schematic of a) detailed ligand atom interactions with the protein residues. Red residue: Negatively charged, Purple residue: Positively charged, White residue: Glycine, Yellow residue: Hydrophobic, Blue residue: Polar, Purple arrow: H-bond, Orange arrow: Halogen Bond, Purple line: Metal coordination, Green line: Pi-Pi stacking, Grey circle: Solvent exposure.and b) Protein-Ligand RMSD analyses of ZINC000299790499 with MiD49 receptor, using Schrödinger Meastro simulation interactions diagram.

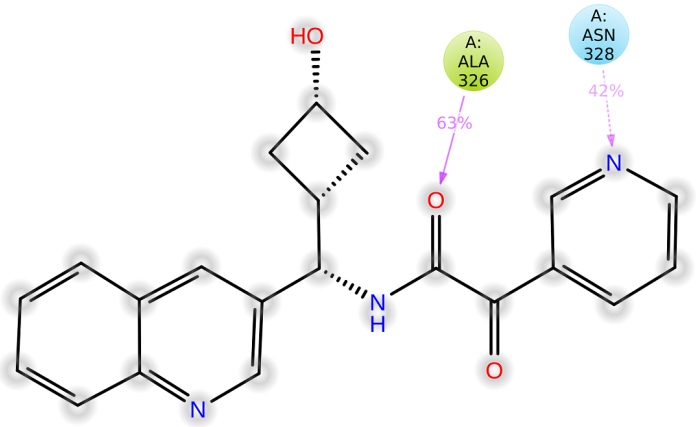

(a)

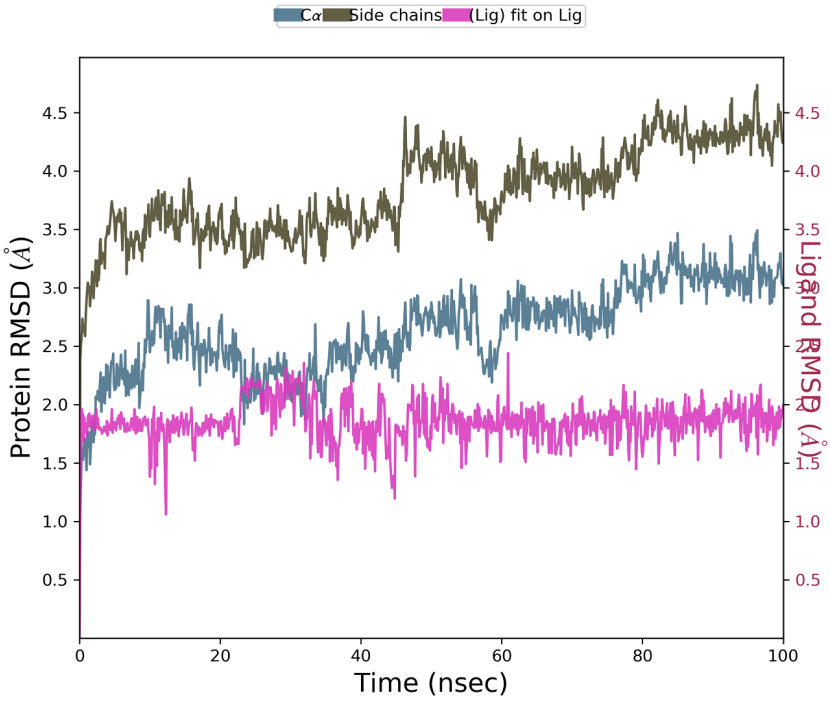

(b)

Figure 3.22 : The schematic of a) detailed ligand atom interactions with the protein residues. Red residue: Negatively charged, Purple residue: Positively charged, White residue: Glycine, Yellow residue: Hydrophobic, Blue residue: Polar, Purple arrow: H-bond, Orange arrow: Halogen Bond, Purple line: Metal coordination, Green line: Pi-Pi stacking, Grey circle: Solvent exposure.and b) Protein-Ligand RMSD analyses of ZINC000244858477 with MiD49 receptor, using Schrödinger Meastro simulation interactions diagram.

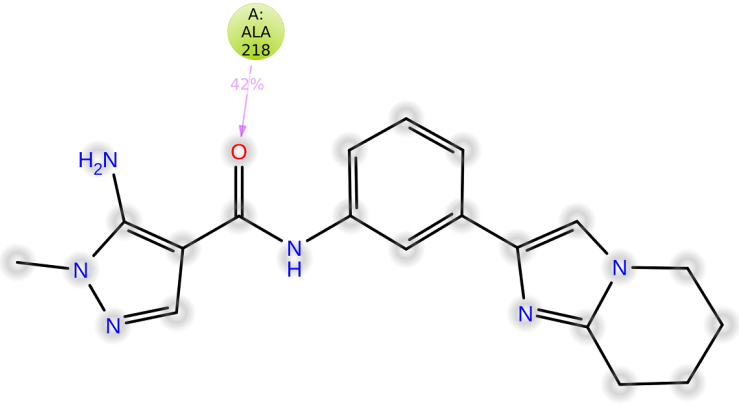

(a)

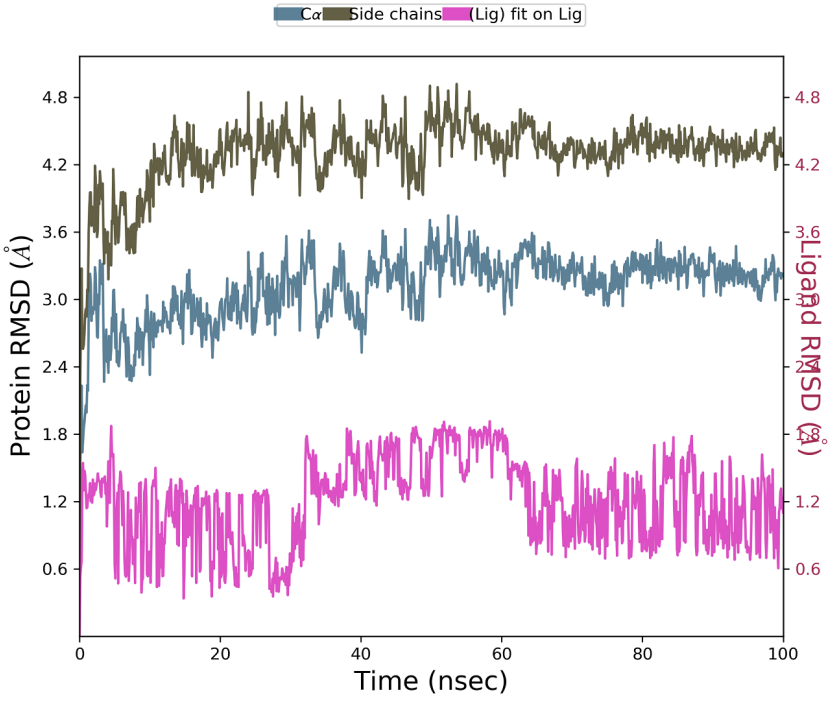

(b)

Figure 3.23 : The schematic of a) detailed ligand atom interactions with the protein residues. Red residue: Negatively charged, Purple residue: Positively charged, White residue: Glycine, Yellow residue: Hydrophobic, Blue residue: Polar, Purple arrow: H-bond, Orange arrow: Halogen Bond, Purple line: Metal coordination, Green line: Pi-Pi stacking, Grey circle: Solvent exposure.and b) Protein-Ligand RMSD analyses of ZINC000097375288 with MiD49 receptor, using Schrödinger Meastro simulation interactions diagram.

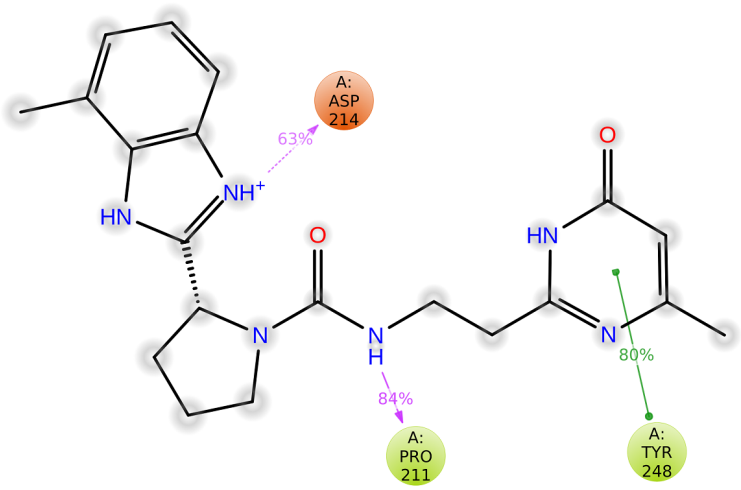

(a)

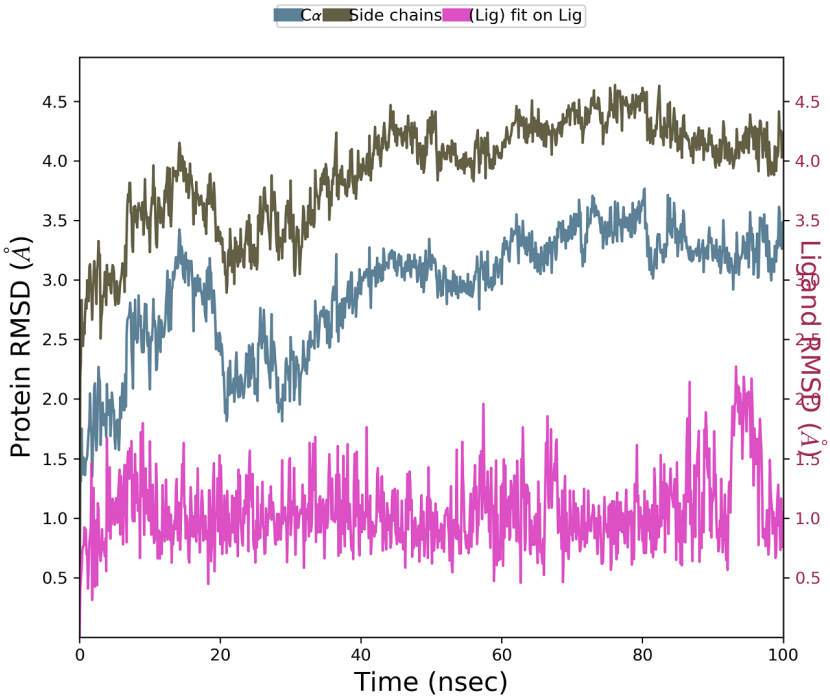

(b)

Figure 3.24 : The schematic of a) detailed ligand atom interactions with the protein residues. Red residue: Negatively charged, Purple residue: Positively charged, White residue: Glycine, Yellow residue: Hydrophobic, Blue residue: Polar, Purple arrow: H-bond, Orange arrow: Halogen Bond, Purple line: Metal coordination, Green line: Pi-Pi stacking, Grey circle: Solvent exposure.and b) Protein-Ligand RMSD analyses of ZINC000426507853 with MiD49 receptor, using Schrödinger Meastro simulation interactions diagram.

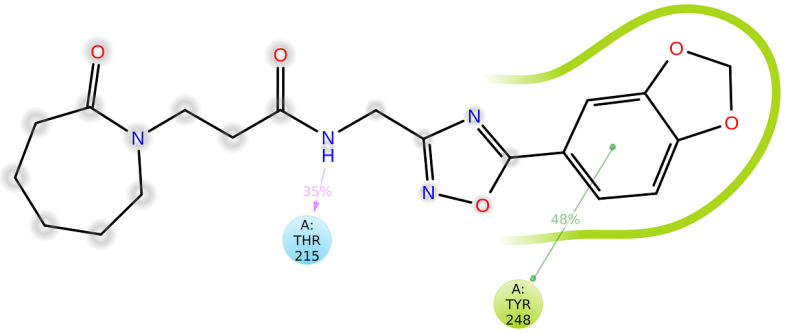

(a)

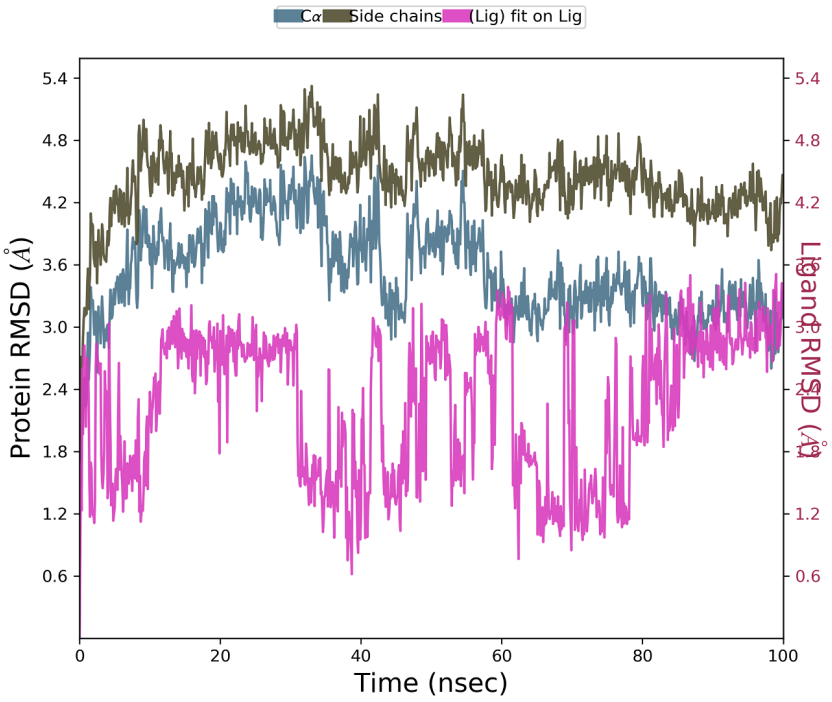

(b)

Figure 3.25 : The schematic of a) detailed ligand atom interactions with the protein residues. Red residue: Negatively charged, Purple residue: Positively charged, White residue: Glycine, Yellow residue: Hydrophobic, Blue residue: Polar, Purple arrow: H-bond, Orange arrow: Halogen Bond, Purple line: Metal coordination, Green line: Pi-Pi stacking, Grey circle: Solvent exposure.and b) Protein-Ligand RMSD analyses of ZINC000952970431 with MiD49 receptor, using Schrödinger Meastro simulation interactions diagram.

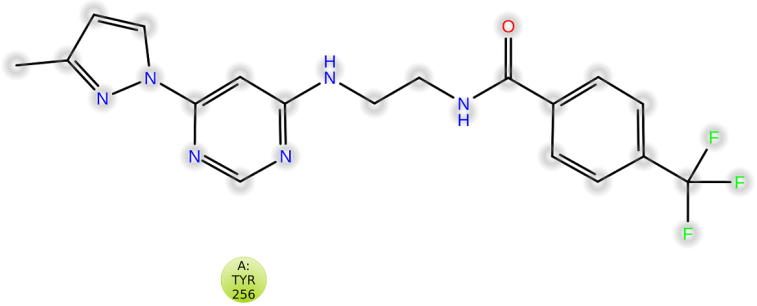

(a)

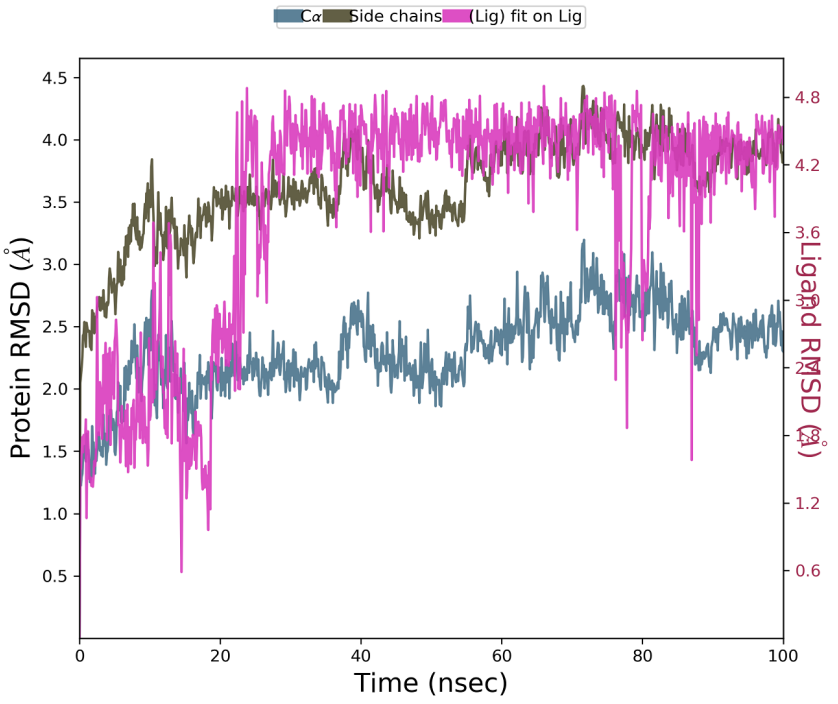

(b)

Figure 3.26 : The schematic of a) detailed ligand atom interactions with the protein residues. Red residue: Negatively charged, Purple residue: Positively charged, White residue: Glycine, Yellow residue: Hydrophobic, Blue residue: Polar, Purple arrow: H-bond, Orange arrow: Halogen Bond, Purple line: Metal coordination, Green line: Pi-Pi stacking, Grey circle: Solvent exposure.and b) Protein-Ligand RMSD analyses of ZINC000072441507 with MiD49 receptor, using Schrödinger Meastro simulation interactions diagram.

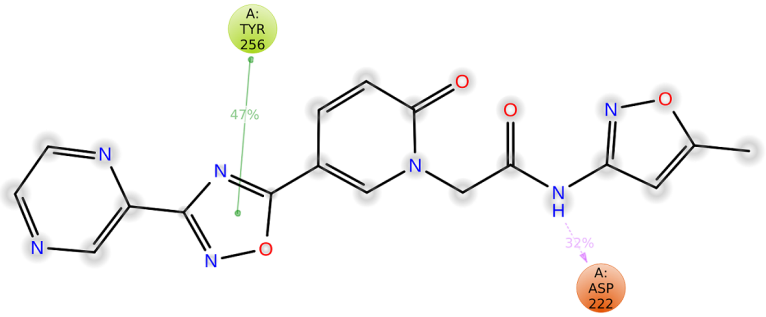

(a)

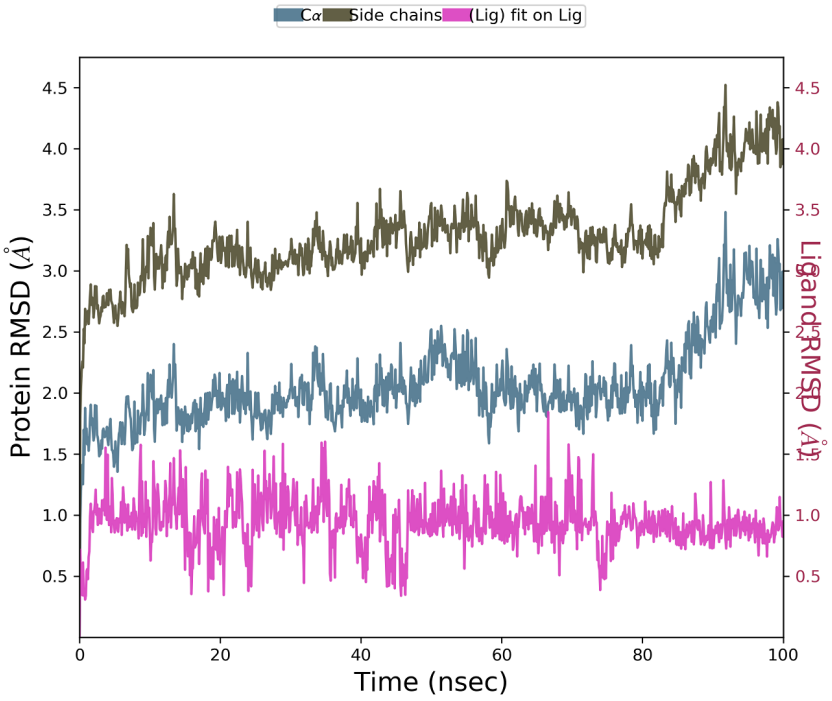

(b)

Figure 3.27 : The schematic of a) detailed ligand atom interactions with the protein residues. Red residue: Negatively charged, Purple residue: Positively charged, White residue: Glycine, Yellow residue: Hydrophobic, Blue residue: Polar, Purple arrow: H-bond, Orange arrow: Halogen Bond, Purple line: Metal coordination, Green line: Pi-Pi stacking, Grey circle: Solvent exposure.and b) Protein-Ligand RMSD analyses of ZINC000077199968 with MiD49 receptor, using Schrödinger Meastro simulation interactions diagram.

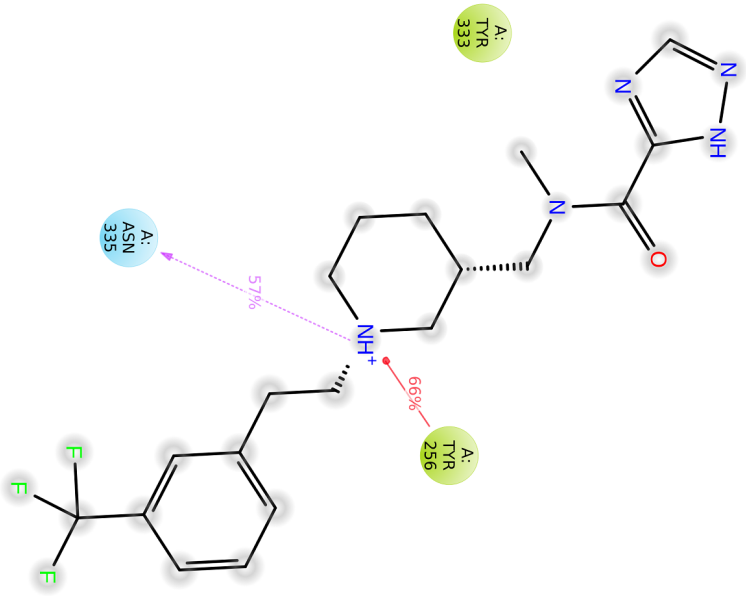

(a)

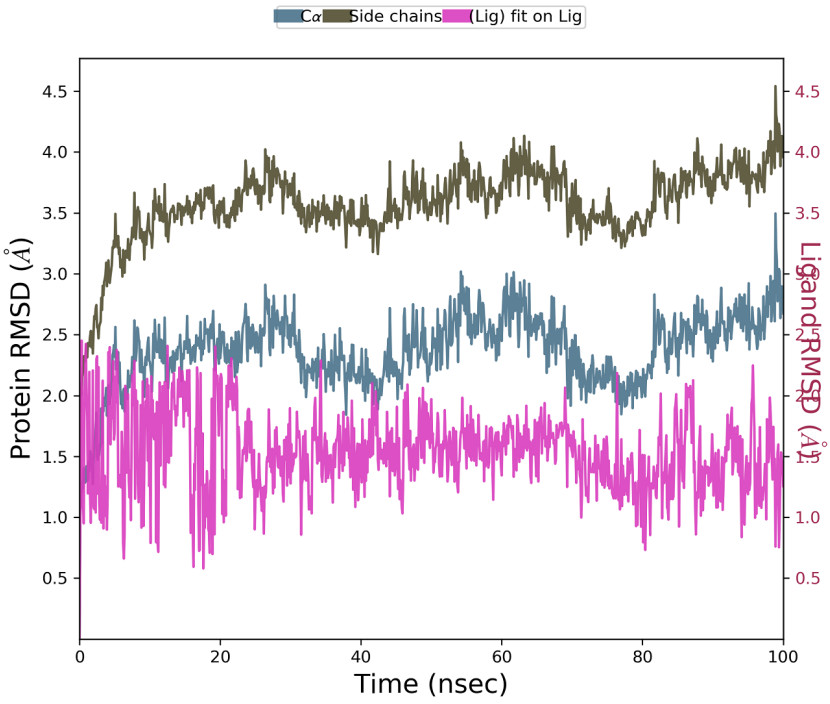

(b)

Figure 3.28 : The schematic of a) detailed ligand atom interactions with the protein residues. Red residue: Negatively charged, Purple residue: Positively charged, White residue: Glycine, Yellow residue: Hydrophobic, Blue residue: Polar, Purple arrow: H-bond, Orange arrow: Halogen Bond, Purple line: Metal coordination, Green line: Pi-Pi stacking, Grey circle: Solvent exposure.and b) Protein-Ligand RMSD analyses of ZINC000095524021 with MiD49 receptor, using Schrödinger Meastro simulation interactions diagram.

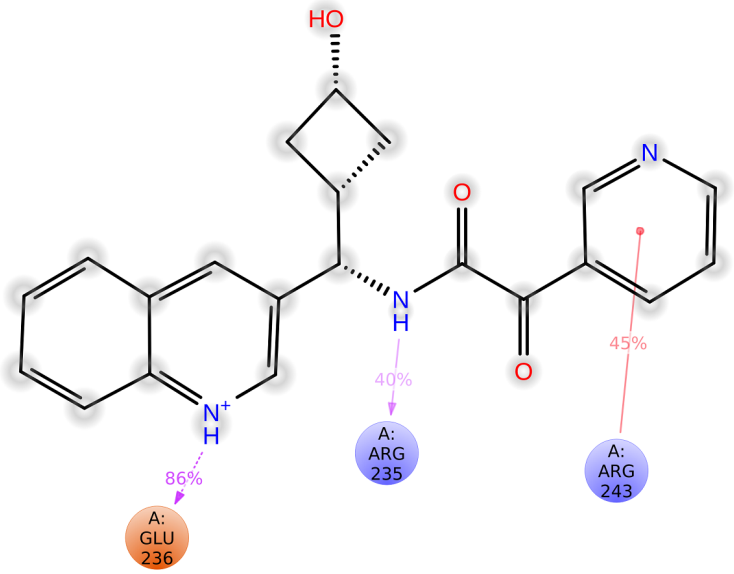

(a)

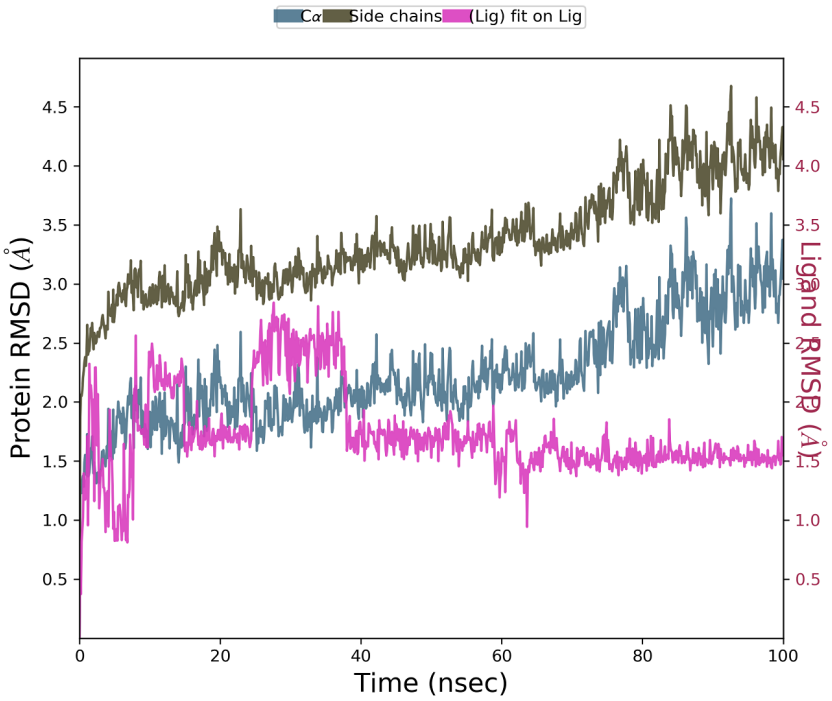

(b)

Figure 3.29 : The schematic of a) detailed ligand atom interactions with the protein residues. Red residue: Negatively charged, Purple residue: Positively charged, White residue: Glycine, Yellow residue: Hydrophobic, Blue residue: Polar, Purple arrow: H-bond, Orange arrow: Halogen Bond, Purple line: Metal coordination, Green line: Pi-Pi stacking, Grey circle: Solvent exposure.and b) Protein-Ligand RMSD analyses of ZINC000244858477 with MiD49 receptor, using Schrödinger Meastro simulation interactions diagram.

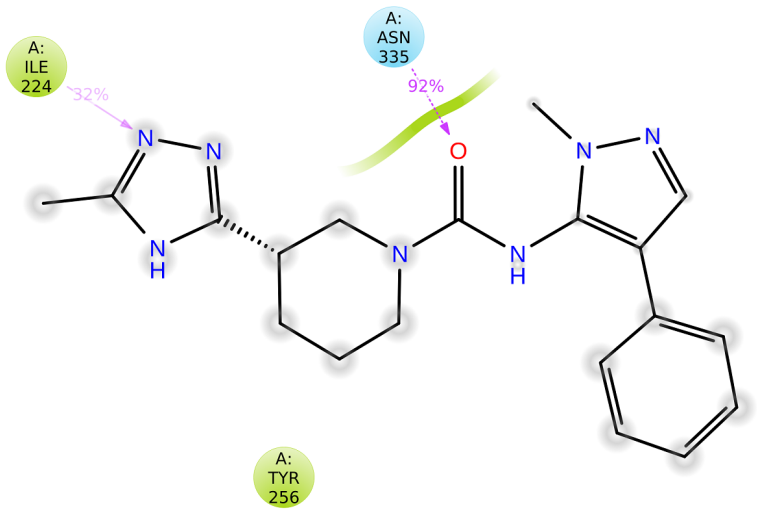

(a)

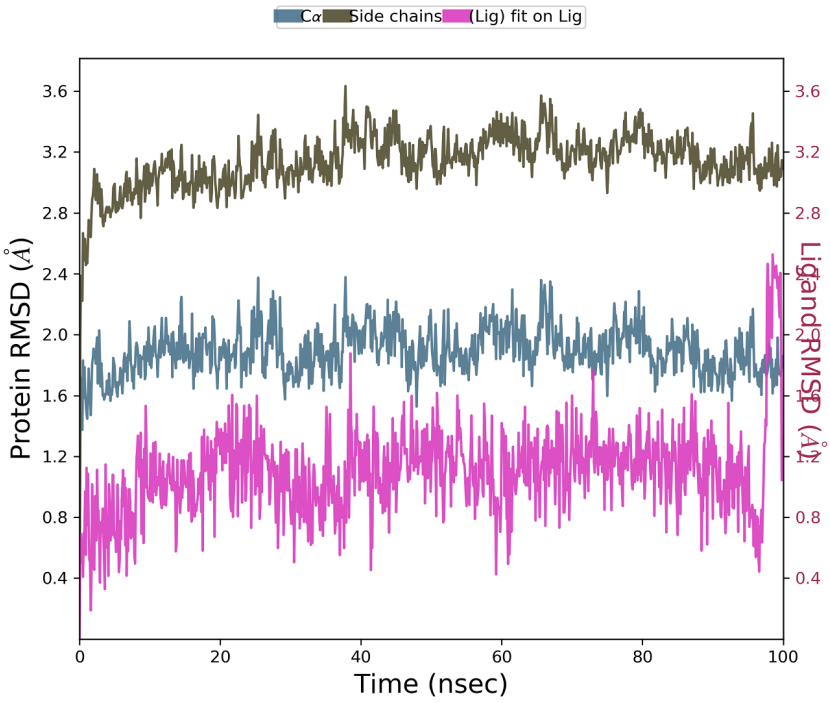

(b)

Figure 3.30 : The schematic of a) detailed ligand atom interactions with the protein residues. Red residue: Negatively charged, Purple residue: Positively charged, White residue: Glycine, Yellow residue: Hydrophobic, Blue residue: Polar, Purple arrow: H-bond, Orange arrow: Halogen Bond, Purple line: Metal coordination, Green line: Pi-Pi stacking, Grey circle: Solvent exposure.and b) Protein-Ligand RMSD analyses of ZINC000299757959 with MiD49 receptor, using Schrödinger Meastro simulation interactions diagram.

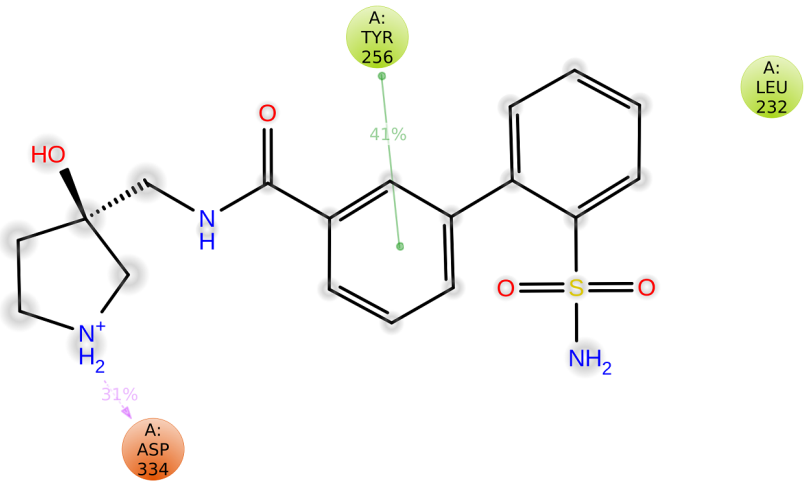

(a)

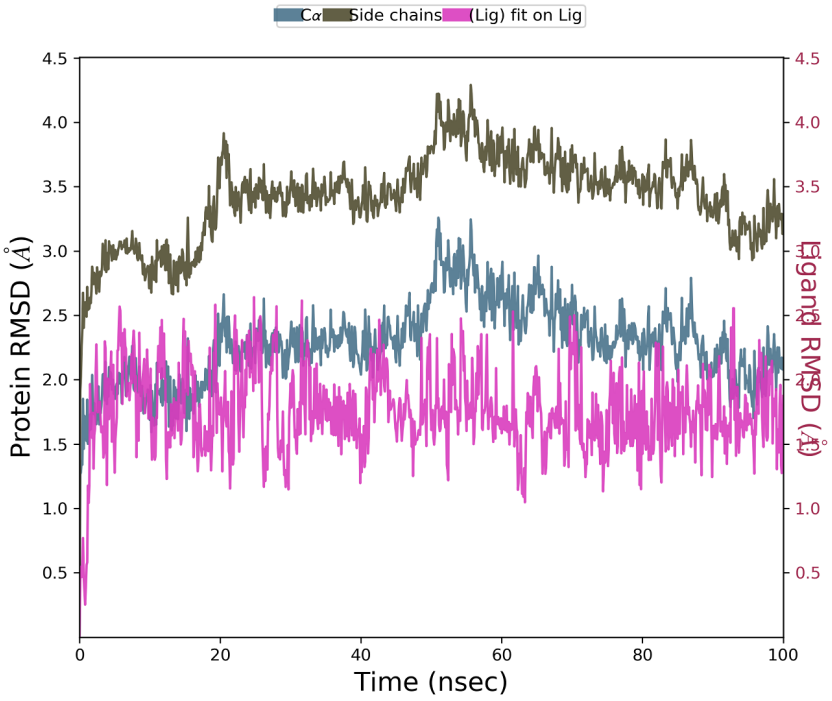

(b)

Figure 3.31 : The schematic of a) detailed ligand atom interactions with the protein residues. Red residue: Negatively charged, Purple residue: Positively charged, White residue: Glycine, Yellow residue: Hydrophobic, Blue residue: Polar, Purple arrow: H-bond, Orange arrow: Halogen Bond, Purple line: Metal coordination, Green line: Pi-Pi stacking, Grey circle: Solvent exposure.and b) Protein-Ligand RMSD analyses of ZINC000426379642 with MiD49 receptor, using Schrödinger Meastro simulation interactions diagram.

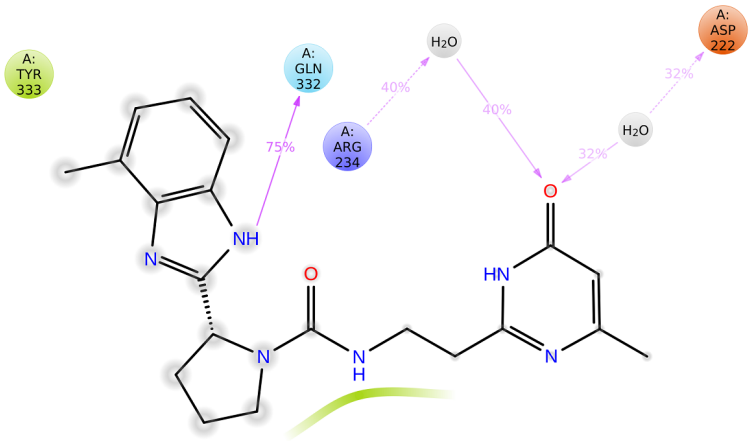

(a)

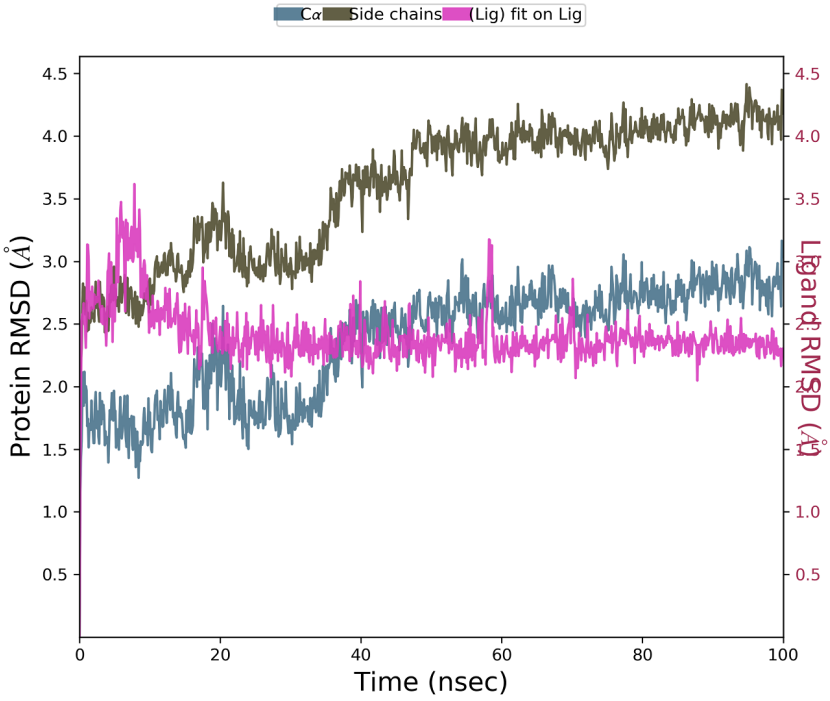

(b)

Figure 3.32 : The schematic of a) detailed ligand atom interactions with the protein residues. Red residue: Negatively charged, Purple residue: Positively charged, White residue: Glycine, Yellow residue: Hydrophobic, Blue residue: Polar, Purple arrow: H-bond, Orange arrow: Halogen Bond, Purple line: Metal coordination, Green line: Pi-Pi stacking, Grey circle: Solvent exposure.and b) Protein-Ligand RMSD analyses of ZINC000426507853 with MiD49 receptor, using Schrödinger Meastro simulation interactions diagram.

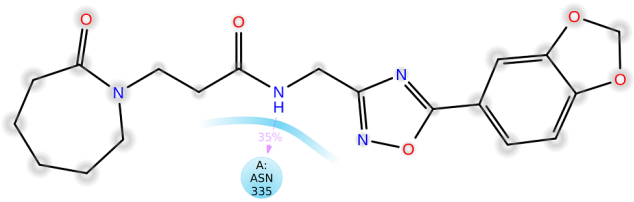

(a)

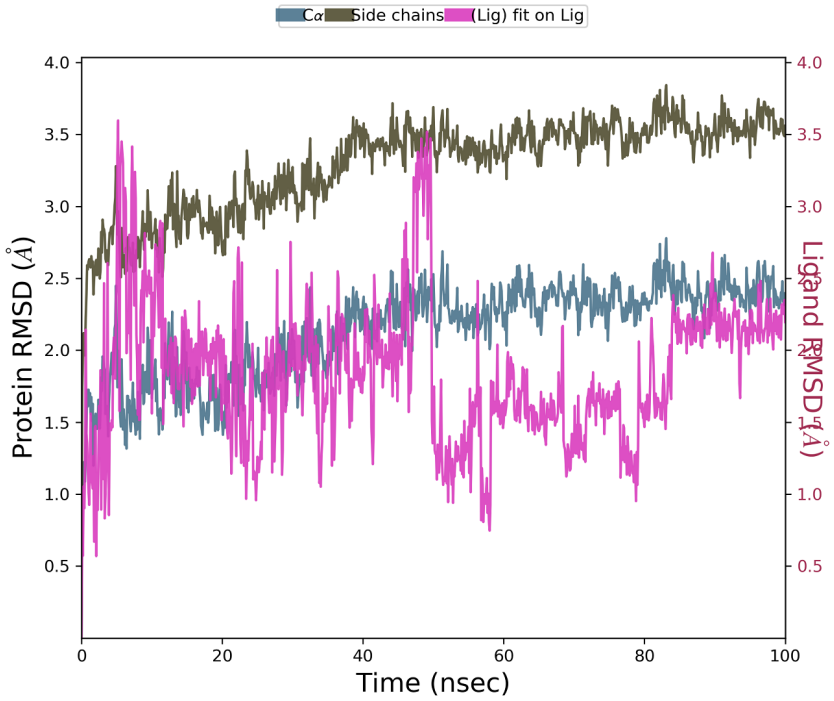

(b)

Figure 3.33 : The schematic of a) detailed ligand atom interactions with the protein residues. Red residue: Negatively charged, Purple residue: Positively charged, White residue: Glycine, Yellow residue: Hydrophobic, Blue residue: Polar, Purple arrow: H-bond, Orange arrow: Halogen Bond, Purple line: Metal coordination, Green line: Pi-Pi stacking, Grey circle: Solvent exposure.and b) Protein-Ligand RMSD analyses of ZINC000952970431 with MiD49 receptor, using Schrödinger Meastro simulation interactions diagram.

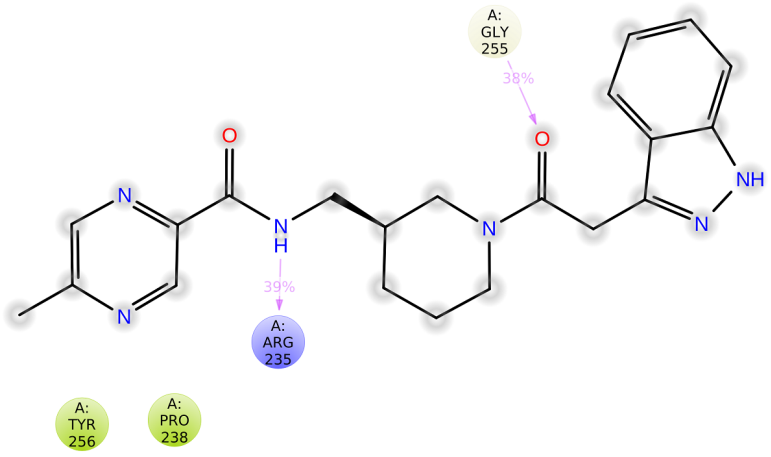

(a)

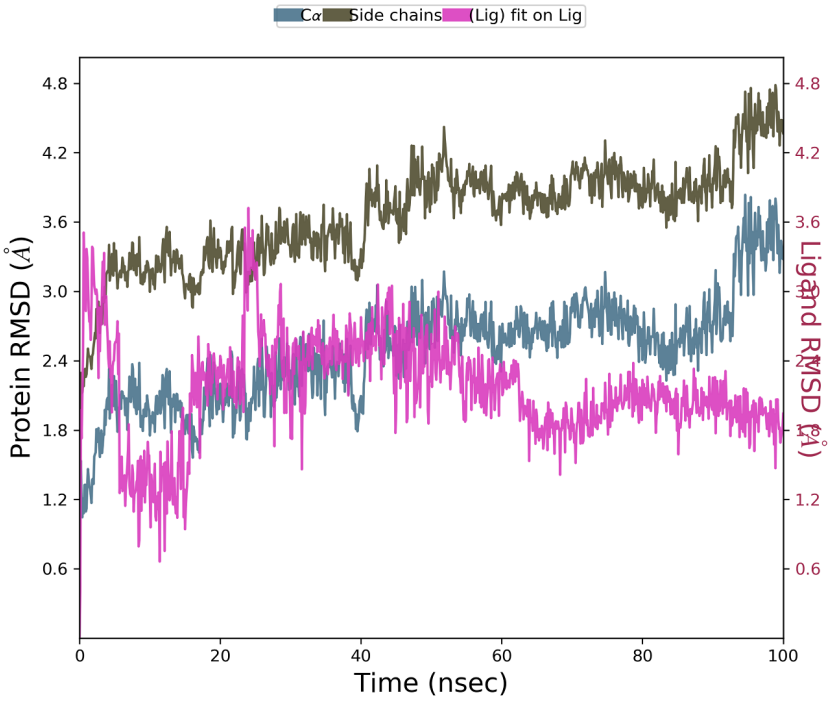

(b)

Figure 3.34 : The schematic of a) detailed ligand atom interactions with the protein residues. Red residue: Negatively charged, Purple residue: Positively charged, White residue: Glycine, Yellow residue: Hydrophobic, Blue residue: Polar, Purple arrow: H-bond, Orange arrow: Halogen Bond, Purple line: Metal coordination, Green line: Pi-Pi stacking, Grey circle: Solvent exposure.and b) Protein-Ligand RMSD analyses of ZINC000952972711 with MiD49 receptor, using Schrödinger Meastro simulation interactions diagram.

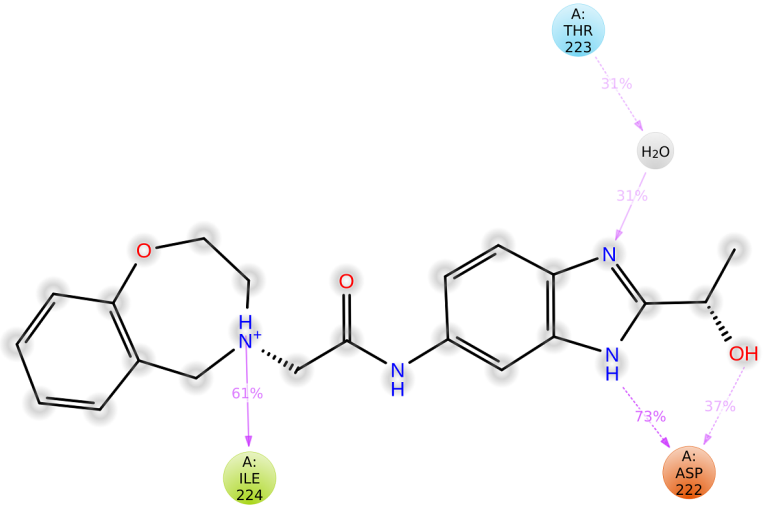

(a)

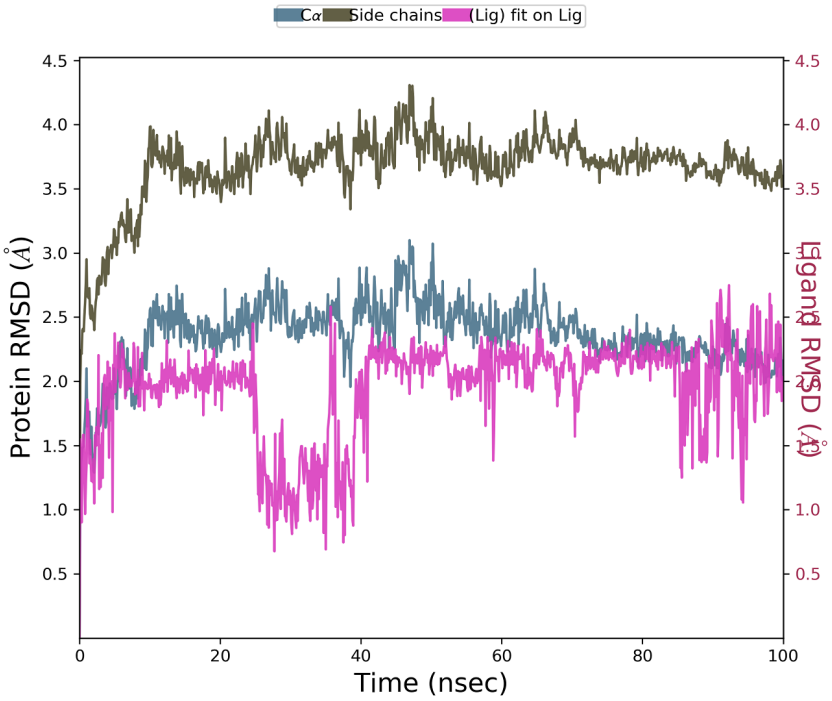

(b)

Figure 3.35 : The schematic of a) detailed ligand atom interactions with the protein residues. Red residue: Negatively charged, Purple residue: Positively charged, White residue: Glycine, Yellow residue: Hydrophobic, Blue residue: Polar, Purple arrow: H-bond, Orange arrow: Halogen Bond, Purple line: Metal coordination, Green line: Pi-Pi stacking, Grey circle: Solvent exposure.and b) Protein-Ligand RMSD analyses of ZINC000952975679 with MiD49 receptor, using Schrödinger Meastro simulation interactions diagram.

4. Conclusion

In this thesis, a technique based on molecular docking is offered to predict new potential drug molecules as the inhibitors for Drp1-MiD49/51 interaction.

Docking calculations were carried out in phases to achieve this purpose. The ZINC database was utilized to start docking calculations using 3.5 million in-stock lead-like small molecules. Then the high-scoring molecules from the preceding stage were docked into candidate off-target proteins, as well as to the target proteins. Thereafter, molecules with particular criteria were chosen for docking using Glide XP, followed by clustering and ADME/T characteristics to choose the best ligands for pharmaceutical usage. Ultimately, the high-scored compounds from the preceding stage were chosen for molecular dynamic simulations. The compounds with the highest scores were chosen as the top 30 for the studies of experimental phase of the work.

Results of first stage and second stage screening as well as extra precision docking calculations using Glide for our library of small molecules showed that docking of small molecules to our target proteins: Drp1, MiD49 and MiD51 yielded high binding scores, indicating that selected ligands can bind into our target proteins with high affinity. In this step, we reduced the big library of ligands to 200 high scored molecules and performed a clustering analysis for them to eliminate molecules with similar structures in order to eliminate molecules with similar chemical activities. The outcomes of clustering fingerprinting indicated that top ligand candidates differ in chemical and structural features. This diversity allows a greater number of molecules to be tested experimentally in future investigations. After clustering analysis came ADME/T analysis which let us find molecules with not only having high affinity against our target proteins, but also show appropriate ADMET properties at a therapeutic dose. In this regard we performed an ADME/T analysis after clustering analysis and the best resulted molecules were selected. ADME/T analyses results demonstrated that our candidate ligands are statistically closer to optimum in terms

of drug-likeness and pharmaceutical characteristics. In this step, a MD simulation was carried out for candidate molecules and RMSD and Protein-Ligand interaction analyses were performed. RMSD results depicts the rigidity and stability of our ligands within protein-ligand complex, according to analyses of top-scored ligand displacement trajectories against Drp1, MiD49, and MiD51. This indicates that the majority of our candidate ligands are stable within the complex and can properly remain within the binding pocket of target protein. According to the studies, RMSD range between 1.0 and 3.0 indicates that atom displacements are negligible, and consequently the overall stability of the protein and ligands was kept in the bound complex. Target proteins were seen to be highly stable over the course of simulation in the majority of MD simulations for ligand-bound complexes. Protein RMSD fluctuations were generally smaller than 2.5-3.0, which is considered acceptable.

REFERENCES

[1] **Meng, X.Y.**, **Zhang, H.X.**, **Mezei, M. and Cui, M.** (2011). Molecular docking: a powerful approach for structure-based drug discovery, *Current computer-aided drug design*, *7*(2), 146–157.

[2] **Maia, E.H.B.**, **Assis, L.C.**, **De Oliveira, T.A.**, **Da Silva, A.M. and Taranto, A.G.** (2020). Structure-based virtual screening: from classical to artificial intelligence, *Frontiers in chemistry*, *8*, 343.

[3] **Trott, O. and Olson, A.J.** (2010). AutoDock Vina: improving the speed and accuracy of docking with a new scoring function, efficient optimization, and multithreading, *Journal of computational chemistry*, *31*(2), 455–461.

[4] **Liu, N. and Xu, Z.** (2019). Using LeDock as a docking tool for computational drug design, *IOP Conference Series: Earth and Environmental Science*, volume218, IOP Publishing, p.012143.

[5] **Friesner, R.A.**, **Murphy, R.B.**, **Repasky, M.P.**, **Frye, L.L.**, **Greenwood, J.R.**, **Halgren, T.A.**, **... and Mainz, D.T.** (2006). Extra precision glide: Docking and scoring incorporating a model of hydrophobic enclosure for protein-ligand complexes, *Journal of medicinal chemistry*, *49*(21), 6177–6196.

[6] **Wallace, D.C.** (1999). Mitochondrial diseases in man and mouse, *Science*, *283*(5407), 1482–1488.

[7] **Kannan, K. and Jain, S.K.** (2000). Oxidative stress and apoptosis, *Pathophysiology*, *7*(3), 153–163.

[8] **Yang, Y.**, **Ouyang, Y.**, **Yang, L.**, **Beal, M.F.**, **McQuibban, A.**, **Vogel, H. and Lu, B.** (2008). Pink1 regulates mitochondrial dynamics through interaction with the fission/fusion machinery, *Proceedings of the National Academy of Sciences*, *105*(19), 7070–7075.

[9] **Brown, G.C.**, **Murphy, M.P.**, **Scott, I. and Youle, R.J.** (2010). Mitochondrial fission and fusion, *Essays in biochemistry*, *47*, 85–98.

[10] **Dai, W. and Jiang, L.** (2019). Dysregulated mitochondrial dynamics and metabolism in obesity, diabetes, and cancer, *Frontiers in endocrinology*, 570.

[11] **Kunkel, G.H.**, **Chaturvedi, P. and Tyagi, S.C.** (2015). Epigenetic revival of a dead cardiomyocyte through mitochondrial interventions, *Biomolecular concepts*, *6*(4), 303–319.

[12] **Senft, D. and Ze'ev, A.R.** (2016). Regulators of mitochondrial dynamics in cancer, *Current opinion in cell biology*, *39*, 43–52.

[13] **Rhodes, D.R.**, **Yu, J.**, **Shanker, K.**, **Deshpande, N.**, **Varambally, R.**, **Ghosh, D.**, **Barrette, T.**, **... and Chinnaiyan, A.M.** (2004). ONCOMINE: a cancer microarray database and integrated data-mining platform, *Neoplasia*, *6*(1), 1–6.

[14] **Yu, L.**, **Xiao, Z.**, **Tu, H.**, **Tong, B. and Chen, S.** (2019). The expression and prognostic significance of Drp1 in lung cancer: a bioinformatics analysis and immunohistochemistry, *Medicine*, *98*(48).

[15] **Francy, C.A.**, **Clinton, R.W.**, **Fröhlich, C.**, **Murphy, C. and Mears, J.A.** (2017). Cryo-EM studies of Drp1 reveal cardiolipin interactions that activate the helical oligomer, *Scientific reports*, *7*(1), 1–12.

[16] **Wada, J. and Nakatsuka, A.** (2016). Mitochondrial dynamics and mitochondrial dysfunction in diabetes, *Acta Medica Okayama*, *70*(3), 151–158.

[17] **Palmer, C.S.**, **Elgass, K.D.**, **Parton, R.G.**, **Osellame, L.D.**, **Stojanovski, D. and Ryan, M.T.** (2013). Adaptor proteins MiD49 and MiD51 can act independently of Mff and Fis1 in Drp1 recruitment and are specific for mitochondrial fission, *Journal of Biological Chemistry*, *288*(38), 27584–27593.

[18] **Yapa, N.M.**, **Lisnyak, V.**, **Reljic, B. and Ryan, M.T.** (2021). Mitochondrial dynamics in health and disease, *FEBS letters*, *595*(8), 1184–1204.

[19] **Losón, O.C.**, **Meng, S.**, **Ngo, H.**, **Liu, R.**, **Kaiser, J.T. and Chan, D.C.** (2015). Crystal structure and functional analysis of MiD49, a receptor for the mitochondrial fission protein Drp1, *Protein Science*, *24*(3), 386–394.

[20] **Pettersen, E.F.**, **Goddard, T.D.**, **Huang, C.C.**, **Couch, G.S.**, **Greenblatt, D.M.**, **Meng, E.C. and Ferrin, T.E.** (2004). UCSF Chimera—a visualization system for exploratory research and analysis, *Journal of computational chemistry*, *25*(13), 1605–1612.

[21] **Schrödinger, L. and DeLano, W.** *PyMOL*, `http://www.pymol.org/pymol`.

[22] **Frohlich, C.**, **Grabiger, S.**, **Schwefel, D.**, **Faelber, K.**, **Rosenbaum, E.**, **Mears, J.**, **Rocks, O. and Daumke, O.** (2013). Structural insights into oligomerization and mitochondrial remodelling of dynamin 1-like protein, *The EMBO journal*, *32*(9), 1280–1292.

[23] **Dill, K.A.**, **Bromberg, S.**, **Yue, K.**, **Chan, H.S.**, **Ftebig, K.M.**, **Yee, D.P. and Thomas, P.D.** (1995). Principles of protein folding—a perspective from simple exact models, *Protein science*, *4*(4), 561–602.

[24] **Richter, V.**, **Palmer, C.S.**, **Osellame, L.D.**, **Singh, A.P.**, **Elgass, K.**, **Stroud, D.A.**, **... and Ryan, M.T.** (2014). Structural and functional analysis of MiD51, a dynamin receptor required for mitochondrial fission, *Journal of Cell Biology*, *204*(4), 477–486.

[25] **Berman, H.M.**, **Westbrook, J.**, **Feng, Z.**, **Gilliland, G.**, **Bhat, T.N.**, **Weissig, H.**, **... and Bourne, P.E.** (2000). The protein data bank, *Nucleic acids research*, *28*(1), 235–242.

[26] **Irwin, J.J. and Shoichet, B.K.** (2005). ZINC- a free database of commercially available compounds for virtual screening, *Journal of chemical information and modeling*, *45*(1), 177–182.

[27] **Open Babel development team**. *Open Babel*, `http://openbabel.org/wiki/Main_Page`.

[28] **Altschul, S.F.**, **Gish, W. and Miller, W.** (1990). Myers, tj, *W. &k Lipman, D.. I*, 403–410.

[29] **Schwede, T.**, **Kopp, J.**, **Guex, N. and Peitsch, M.C.** (2003). SWISS-MODEL: an automated protein homology-modeling server, *Nucleic acids research*, *31*(13), 3381–3385.

[30] **Konc, J. and Janežič, D.** (2010). ProBiS: a web server for detection of structurally similar protein binding sites, *Nucleic acids research*, *38*(suppl_2), W436–W440.

[31] **Ayoub, R. and Lee, Y.** (2017). RUPEE: Scalable protein structure search using run position encoded residue descriptors, *Bioinformatics and Biomedicine (BIBM), 2017 IEEE International Conference on*.

[32] **Holm, L.**, (2020). Using Dali for protein structure comparison, Structural Bioinformatics, Springer, pp.29–42.

[33] **Rose, P.W.**, **Bi, C.**, **Bluhm, W.F.**, **Christie, C.H.**, **Dimitropoulos, D.**, **Dutta, S.**, **...** *et al.* (2012). The RCSB Protein Data Bank: new resources for research and education, *Nucleic acids research*, *41*(D1), D475–D482.

[34] **Carpentier, M.**, **Brouillet, S. and Pothier, J.** (2005). YAKUSA: a fast structural database scanning method, *Proteins: Structure, Function, and Bioinformatics*, *61*(1), 137–151.

[35] **Sud, M.** (2016). MayaChemTools: an open source package for computational drug discovery, *Journal of chemical information and modeling*, *56*(12), 2292–2297.

[36] **O'Boyle, N.M.**, **Banck, M.**, **James, C.A.**, **Morley, C.**, **Vandermeersch, T. and Hutchison, G.R.** (2011). Open Babel: An open chemical toolbox, *Journal of cheminformatics*, *3*(1), 1–14.

CURRICULUM VITAE

Name Surname **:** Behnaz Ghaderkalankesh

EDUCATION :

- **B.Sc. :**2015, Islamic Azad University, Faculty of Engineering, Information Technology
- **M.Sc.:**Present, Istanbul Technical University